

# Persistence of a reef fish metapopulation via network connectivity: theory and data

Allison G. Dedrick<sup>a,\*</sup>,<sup>1</sup>

Katrina A. Catalano<sup>a</sup>

Michelle R. Stuart<sup>a</sup>

J. Wilson White<sup>b</sup>

Humberto Montes, Jr.<sup>c</sup>

Malin Pinsky<sup>a</sup>

a. Department of Ecology Evolution and Natural Resources, Rutgers University, 14 College Farm Road, New Brunswick, NJ 08901 USA;

b. Department of Fisheries and Wildlife, Coastal Oregon Marine Experiment Station, Oregon State University, Newport, OR 97365 USA;

c. Visayas State University

\* Corresponding author; e-mail: agdedrick@gmail.com

1. Current address: Stanford Woods Institute for the Environment, Stanford University, Stanford, CA 94305 USA.

# Introduction

Metapopulation dynamics and persistence depend on connectivity among patches and the demographic rates at each patch (e.g. Hastings and Botsford, 2006; Hanski, 1998). Assessing levels of connectivity and demographic parameters has been particularly challenging for marine species, where much of the mortality and movement happens at larval and juvenile stages when individuals are hard to track and have the potential to travel long distances with ocean currents (reviewed in White et al., 2019). A need to understand metapopulations for conservation and management, such as siting marine protected areas (e.g. Botsford et al., 2001; White et al., 2010), however, has led to a large body of theory describing how marine metapopulations might persist.

For any population to persist, individuals must on average replace themselves during their lifetime. Assessing replacement must take into account the demographic processes across the whole life cycle, including how likely individuals are to survive to the next age or stage, their expected fecundity at each stage, and the survival of any offspring produced to recruitment. In a spatially structured population, as many marine populations are, in addition to assessing whether the reproductive output and survival of a population is sufficient, we must also consider how the offspring are distributed across space.

Considering both the demographic processes within patches and the connectivity among them, a metapopulation can persist in two ways: 1) at least one patch can achieve replacement in isolation, or 2) patches receive enough recruitment to achieve

replacement through multi-generational loops of connectivity with other patches in the metapopulation (Hastings and Botsford, 2006; Burgess et al., 2014). In the first case (termed self-persistence), enough of the reproductive output produced at one patch is retained at the patch for it to persist. In the second (network persistence), closed loops of connectivity among at least some of the patches - where individuals from one patch settle at another and eventually send offspring back to the first in a future generation - provide the patch with enough recruitment to persist within the network. Though it has been challenging to estimate the parameters necessary to understand how actual metapopulations persist, a large work of theory developed in part to guide marine protected area design helps predict when each type of persistence is likely to occur (i.e., habitat patches or protected areas that are large relative to the mean dispersal distance are likely to be self-persistent, White et al., 2010).

New ways of identifying individuals and determining their origins, such as otolith and shell microchemistry and genetic parentage analysis (e.g., Wang, 2004, 2014), now allow better measurements of dispersal (e.g., Almany et al., 2017; D'Aloia et al., 2013), and a better appreciation of the relevant population dynamic theory has led to measurement of the appropriate demographic factors (e.g., Carson et al., 2011; Hameed et al., 2016) necessary to assess persistence in real metapopulations. We might expect that populations on isolated islands are the most likely to be self-persistent, as they lack nearby populations with which to exchange larvae and would go locally extinct if they did not achieve replacement. At isolated Kimbe Island in Papua New Guinea, Salles et al. (2015) find that the population of orange clownfish (*Amphiprion percula*) can likely persist without outside immigration. In contrast,

populations of bicolor damselfish (*Stegastes partitus*) at four study sites nested within a larger reef metapopulation in the Bahamas do not appear able to persist without outside input (Johnson et al., 2018). Persistence has yet to be assessed in the field for an entire marine metapopulation, such as all of the patches in a coastal metapopulation.

The number of studies estimating demographic rates and connectivity in marine metapopulations is growing (e.g. Carson et al., 2011; Salles et al., 2015; Johnson et al., 2018; Garavelli et al., 2018), but most use data from one or a few years. Longer data sets enable better estimates of long-term average rates, rather than assuming the demographic and dispersal rates from a particular year or two are representative. Long data sets are also useful for explicitly considering uncertainty, both to assess how well we understand persistence for a population and to assess which parameters contribute most to our uncertainty. Finally, sampling over many years provides abundance trends to compare with persistence metrics.

Here, we further our understanding of metapopulation dynamics in a network of patches along a coastline through a study of yellowtail clownfish (*Amphiprion clarkii*) in the Philippines. We assess persistence for all patches of habitat within a 30 km stretch of coastline, which exceeds estimates of the dispersal spread for this species (Pinsky et al., 2010), suggesting the network is likely to operate as a contained metapopulation. With seven years of annual sampling data, we are able to estimate persistence metrics and replacement over the longer term and investigate abundance through time to compare with the replacement-based persistence metrics. We use our long-term data set from habitat patches on a continuous section of coastline to

understand persistence within a local network. We find that our sites have stable abundances through time but are unlikely to persist as an isolated metapopulation and require immigration from outside patches to persist.

## Methods

### Persistence theory and metrics

For a population to persist, each individual must on average replace itself (e.g. Hastings and Botsford, 2006; Botsford et al., 2019). In non-spatially structured populations, we use criteria such as the average number of recruiting offspring each individual produces during its life (called  $R_0$  when the population is age-structured and density-independent) or the growth rate of the population (such as the dominant eigenvalue  $\lambda$  of an age-structured Leslie matrix) (Caswell, 2001; Burgess et al., 2014). For spatially-structured populations, we must also consider the spatial spread of offspring, often represented through a dispersal kernel or connectivity matrix (Burgess et al., 2014).

We consider four primary metrics to assess whether and how the population is persistent: 1) lifetime recruit production (LRP), to assess whether the population has enough surviving offspring to achieve replacement, 2) self-persistence (SP), to assess whether any individual patch can persist in isolation without input from other patches, 3) network persistence (NP), to assess whether the metapopulation is persistent as a connected unit, and 4) local replacement (LR), as second assessment of whether individuals replace themselves with recruits retained within population. We

explain each metric below in detail. To represent the uncertainty in our estimates, we calculate each metric 1000 times, sampling each input parameter from a distribution that represents the uncertainty in each empirical estimate of demographic rates or connectivity. In our results, we show our best estimate of each persistence metric along with the range of uncertainty values.

### **Lifetime recruit production**

We find the estimated number of recruits an individual recruit will produce (lifetime recruit production: LRP) by multiplying the total number of eggs a recruit-sized individual will produce in its lifetime (lifetime egg production: LEP) by the fraction of those eggs that will survive to become recruits (egg-recruit survival:  $S_e$ ) (Fig. 1):

$$\text{LRP} = \text{LEP} * S_e. \quad (1)$$

If  $\text{LRP} \geq 1$ , the population has the potential for replacement; individuals produce enough surviving offspring, before considering dispersal. If  $\text{LRP} < 1$ , the individuals are not replacing themselves and the population cannot persist without input from outside patches and is a sink habitat within a larger metapopulation (Pulliam, 1988). We use all recruits produced by adults in our population to estimate  $\text{LRP}$ , regardless of where they settle.

## Self-persistence

A patch is able to persist in isolation (self-persistent) if individuals produce enough offspring that survive to recruitment (LRP) and settle in the natal patch ( $i$ , with probability of dispersal  $p_{i,i}$ ) to replace themselves:

$$SP_i = \text{LRP}_i \times p_{i,i}. \quad (2)$$

A patch  $i$  is self-persistent if  $SP_i \geq 1$ . If at least one patch is self-persistent, the metapopulation as a whole is persistent as well (Hastings and Botsford, 2006; Burgess et al., 2014). Our equation for SP is a modification of that used in Burgess et al. (2014), which uses LEP to represent offspring produced and uses local retention (the number of surviving recruits that disperse back to the natal patch divided by the number of eggs produced by the natal patch) to capture egg-recruit survival and dispersal combined:  $\text{LEP} \times \text{local retention} \geq 1$ . We modify this to include egg-recruit survival in the offspring term instead, using LRP in place of LEP.

## Network persistence

Network persistence explicitly considers dispersal of individuals among sites, a critical part of the larval life stage, in addition to the reproduction and survival at each site. We represent dispersal with a dispersal kernel, which relates the likelihood of an individual dispersing to the distance traveled. We find the probabilities of a

recruit dispersing between each set of sites ( $p_{i,j}$ ) by integrating the dispersal kernel over the distances between sites. We then create a realized connectivity matrix  $C$  by multiplying the dispersal probabilities by the expected number of recruits an individual produces:  $C_{i,j} = \text{LRP} \times p_{i,j}$  (Burgess et al., 2014, though we include egg-recruit survival in LRP, rather than in  $p_{i,j}$  as they do). The diagonal entries of  $C$ , where the origin and destination are the same site, are the values of self-persistence for each individual site.

Network persistence evaluates the largest real eigenvalue of the realized connectivity matrix  $\lambda_C$ , which must be at least 1 for the network to persist without outside input:  $\text{NP} = \lambda_C \geq 1$  (e.g. Hastings and Botsford, 2006; White et al., 2010; Burgess et al., 2014).

### Local replacement

Like network persistence, local replacement (LR) assesses whether the population is locally self-sustaining. Rather than considering dispersal explicitly as network persistence does, local replacement modifies LRP to estimate the average number of recruits produced per individual that return to settle within our sites. We estimate LR by multiplying LEP by the proportion of eggs produced that survive and return to recruit at our sites ( $R_e$ ), a modification of egg-recruit survival that implicitly includes dispersal. If  $LR \geq 1$ , individuals produce enough locally-retained offspring to replace themselves and the population can persist in isolation.

$$\text{LR} = \text{LEP} \times R_e. \quad (3)$$

## Study system

We focus on a tropical metapopulation of yellowtail clownfish (*Amphiprion clarkii*, Fig. 2c) on the west coast of Leyte island facing the Camotes Sea in the Philippines (Fig. 2a). Like many clownfish species, yellowtail clownfish have a mutualistic relationship with anemones that house small colonies of fish (Buston, 2003b; Fautin et al., 1992). Yellowtail clownfish are protandrous hermaphrodites and maintain a size-structured hierarchy; within an anemone, the largest fish is the breeding female, the next largest is the breeding male, and any smaller fish are non-breeding juveniles. The fish move up in rank to become breeders only after the larger fish have died. In the tropical patch reef habitat of the Philippines, yellowtail clownfish primarily spawn from November to May, laying clutches of benthic eggs that the parents protect and tend (Ochi, 1989; Holtswarth et al., 2017). Larvae hatch after about six days and spend 7-10 days in the water column before returning to reef habitat to settle in an anemone (Fautin et al., 1992).

Clownfish are particularly well-suited to metapopulation studies due to their limited movement as adults and well-defined patchy habitat. Once fish have settled, they tend to stay within close proximity of their anemones, which are found on reef patches. This makes fish easier to relocate for mark-recapture studies and simplifies the exchange between patches to only dispersal during the larval phase. Patches, whether considered to be the reef patch or the anemone territory of the fish, are discrete and easily delineated (Fig. 2a, b), which makes determining the spatial structure of the metapopulation clear. Additionally, clear patches make it easier

to assess how much of the site has been surveyed. These simplifying characteristics in habitat and fish behavior make clownfish and other similarly territorial reef fish useful model systems for studies of metapopulation dynamics and persistence (e.g. Buston and DAloia, 2013; Salles et al., 2015; Johnson et al., 2018). Our focal species of yellowtail clownfish tends to behave more like larger reef fishes, with wider-ranging territories and stronger swimming abilities (Hattori and Yanagisawa, 1991; Ochi, 1989), than the smaller clownfish *A. percula* commonly used in previous metapopulation studies (e.g. Buston et al., 2011; Salles et al., 2015). As we show later, survival in yellowtail clownfish is also lower than *A. percula* and more similar to other damselfishes.

### Field data collection

We focus on a set of nineteen patch reef sites spanning 30 km along the western coast of Leyte island (Fig. 2a). The sites consist of rocky patches of coral reef separated by sand flats, with reef patches covering approximately 20% of the sampling region (Fig. 2b). On the north edge, the sites are isolated from nearby habitat with no substantial reef habitat for at least 20 km.

Since 2012, we have sampled fish and habitat at most of the sites annually (Table A2). During sampling, divers using SCUBA and tethered to GPS readers swam the extent of each site and visited each anemone inhabited by yellowtail clownfish. At each anemone, the divers attempted to catch all of the yellowtail clownfish 3.5 cm and larger, took a small tail fin-clip from each for use in genetic analysis, measured the fork length, noted the tail color (as an indicator of life stage), and tagged the anemone

if not already tagged. Starting in the 2015 field season, fish 6.0 cm and larger were also tagged with a passive integrated transponder (PIT) tag, unless already tagged. Divers also looked for eggs around each anemone and measured and photographed any clutches found. In total, we took fin clips from and genotyped 2407 fish and PIT-tagged 1930 fish across all years and sites combined, marking 3053 individual fish.

## Estimating demographic and dispersal parameters from empirical data

### Parentage analysis and dispersal kernel

Over seven years of sampling, we genotyped 1719 potential parents and 785 juveniles and found 62 parent-offspring matches (details in Catalano et al., in prep). We used a distance-based dispersal kernel fit from the parent-offspring matches (Catalano et al., in prep), where the relative dispersal  $p(d)$  is a function of distance  $d$  in kilometers and parameters  $\theta = 1.19$  and  $z = e^{k_d=-2.33}$  that control the shape and scale of the kernel:  $p(d) = ze^{-(zd)^\theta}$ . The dispersal kernel estimates the relative dispersal by distance for fish that have survived and recruited so does not estimate pre-settlement mortality. To find the probability of fish dispersing among our sites, we numerically integrated the dispersal kernel using the distance from the middle of the origin site ( $i$ ) to the closest ( $d_1$ ) and farthest ( $d_2$ ) bounds of the destination site ( $j$ ):

$$p_{i,j}(d) = \int_{d_1}^{d_2} ze^{-(zd)^\theta} dd. \quad (4)$$

To account for uncertainty in the dispersal kernel, we used sets of the shape parameter  $\theta$  and the scale parameter  $k_d$  that represent the span of the 95% confidence interval when  $k_d$  and  $\theta$  are estimated jointly (Catalano et al., in prep).

### Growth and survival: mark-recapture analyses

We marked fish with both genetic samples and PIT tags, allowing us to estimate growth and survival through mark-recapture. In total, we had 3053 marked fish with size and stage data for each capture time.

For growth, we estimated the parameters of a von Bertalanffy growth curve (Fabens, 1965) in the growth increment form relating the length at first capture  $L_t$  to the length at a later capture  $L_{t+1}$  (Hart and Chute, 2009), where  $L_\infty$  is the average asymptotic size across the population and  $K$  controls the rate of growth:

$$\begin{aligned} L_{t+1} &= L_t + (L_\infty - L_t)[1 - e^{(-K)}] \\ &= e^{(-K)}L_t + L_\infty[1 - e^{(-K)}]. \end{aligned} \tag{5}$$

We see from eqn. 5 that we would expect the first length  $L_t$  and the second length  $L_{t+1}$  to be related linearly (Hart and Chute, 2009). From the slope  $m = e^{(-K)}$  and y-intercept  $b = L_\infty[1 - e^{(-K)}]$ , we calculated the von Bertalanffy parameters, such that  $K = -\ln m$  and  $L_\infty = \frac{b}{(1-m)}$ . We used the first and second capture lengths for fish that were recaptured after a year (within 345 to 385 days) to estimate  $L_\infty$  and  $K$ . For fish recaptured more than two times, we randomly selected only one pair

of recaptures from each to use to estimate the parameters 1000 times. We found the mean estimates and mean standard error of those fits, then sampled from within than range to generate a set of von Bertalanffy growth curves to use in our metric uncertainty calculations.

We used the full set of marked fish to estimate annual survival  $\phi$  and probability of recapture  $p_r$  using the mark-recapture program MARK implemented in R through the package **RMark** (Laake, 2013). We fit several models with year, size, and site effects on the probability of survival on a log-odds scale (see full list in Table A4). For fish that were not recaptured in a particular year, we estimated their size using our growth model (eqn. 5) and the size recorded or estimated in the previous year. Fish are not well-mixed at our sites and divers needed to swim near an anemone to have a reasonable chance of capturing the fish on it so we also considered a distance effect on recapture probability (B.4. We compared the fit of the models using a modified version of the Akaike information criterion that reduces the potential for overfitting with small sample sizes (AICc) and selected the model with the lowest AICc value (Table A4).

## Fecundity

We used a size-dependent fecundity relationship determined using photos of egg clutches and females (Yawdoszyn, in prep), where the number of eggs per clutch ( $E_c$ ) is exponentially related to the length in cm of the female ( $L$ ) with size effect  $\beta_l = 2.388$ , intercept  $b = 1.174$ , and egg age effect  $\beta_e = -0.608$  dependent on if the eggs are old enough to have visible eyes. We multiplied the number of eyed eggs per

clutch by the number of clutches per year  $c_e = 11.9$  (estimate from Holtswarth et al., 2017) to get total annual fecundity  $f$  of a female of length  $L$ :

$$f = c_e * e^{\beta_l \ln(L) + \beta_e [\text{eyed}] + b}. \quad (6)$$

### Lifetime egg production

We used an integral projection model (IPM) (Ellner et al., 2016) with size as the continuous structuring trait  $z$  to estimate lifetime egg production (LEP), the expected total number of eggs produced by one recruit. We initialized the IPM with one recruit-sized individual at the initial annual time step ( $t = 0$ ), then projected forward for 100 time steps. We used the size-dependent survival (eqn. B.5) and growth (eqn. 5) functions as the probability density functions in the kernel to describe the survival and growth of the individual into the next time step. The size distribution ( $v_z$ ) at each time step represents the probability that the individual has survived and grown into each of the possible size categories, ranging from a minimum of  $L_s = 0$  cm to a maximum of  $U_s = 15$  cm divided into 100 equal size bins. The probability that the individual is still alive and of any size decreases as the time steps progress; by using a large number of steps, we are able to avoid arbitrarily setting a maximum age and instead let the probabilities become essentially zero.

We then multiplied the size-distribution  $v_z$  at each time by the size-dependent fecundity  $f_z$  (eqn. 6) to get the total number of eggs produced at each time step. Integrating across time and size gives the total number of eggs one individual is likely to produce in its lifetime:

$$\text{LEP} = \int_{t=0}^{100} \int_{z=L_s}^{z=U_s} v_{z,t} f_z dz dt. \quad (7)$$

When entering the starting individual into the matrix, we use 0.1 as the standard deviation of size to spread the starting individual across size bins. When projecting the distribution of the size of the fish in the next year, we used the size determined by the growth curve (eqn. 5) as the mean along with an estimate of spread to account for differences in fish growth rates. We used our recapture data to estimate the standard deviation ( $\text{size}_{sd}$ ) of the distribution of sizes in the next year of fish starting from one size (Table A1).

We only considered reproductive effort once the fish is female and used the average size of first female observation for recaptured fish as the transition size  $L_f = 9.32\text{cm}$ . To incorporate uncertainty, we sampled directly from the sizes at which recaptured fish were first captured as female (5.2 cm - 12.7 cm) (Fig. 3d).

### Survival from egg to recruit

We estimated survival from egg to recruit ( $S_e$ ) using parentage matches to find the number of surviving recruits produced by genotyped parents (similar to the method in Johnson et al., 2018). We scaled the number offspring we assigned back to parents ( $R_m = 62$ ) by various ways we could have missed offspring in our sampling ( $P_h$ ,  $P_c$ ,  $P_d$ , and  $P_s$ , described below and in Fig. B.1), then divided by the estimated number of eggs produced by genotyped parents (the number of genotyped parents  $N_g = 1719$  multiplied by the expected LEP for a fish of parent size  $\text{LEP}_p$ ):

$$S_e = \frac{\frac{R_m}{P_h P_c P_d P_s}}{N_g \text{LEP}_p}. \quad (8)$$

We scaled the number of matched recruits by the cumulative proportion of habitat in our sites we sampled over time ( $P_h = 0.41$ , details in B.1), the probability of capturing a fish if we sampled its anemone ( $P_c = 0.56$ , see B.2 for details), and the proportion of the total dispersal kernel area from each of our sites covered within our sampling region ( $P_d = 0.57$ , calculation in B.3.0.1). Finally, because our dispersal kernel gives the probability of dispersal given that a recruit settled somewhere but our sampling region is not all habitat, we scaled by the proportion habitat in our sampling region ( $P_s = 0.20$ , details in B.3.0.2) to avoid counting mortality from settling on non-habitat twice.

To estimate the survival and retention of recruits back to our sites for estimating local replacement, we scaled only by the proportion of habitat cumulatively sampled and the probability of capturing a fish:  $R_e = \frac{\frac{R_m}{P_h P_c}}{N_g \text{LEP}_p}$ .

We considered uncertainty in the number of offspring assigned to parents during the parentage analysis ( $R_m$ ) and in the probability of capturing a fish ( $P_c$ ). We generated a set of values for the number of assigned offspring using a random binomial, with the number of genotyped offspring (745) as the number of trials and the assignment rate from the parentage analysis (0.079) as the probability of success on each trial (Catalano et al., in prep). For the probability of capturing a fish, we sampled values from a beta distribution that captures the mean and variance of capture probabilities across recapture dives (details in B.2).

## **Defining recruit and census stage**

When assessing persistence, we must consider mortality and reproduction that occurs across the entire life cycle to determine whether an individual is replacing itself with an individual that reaches the same life stage (Burgess et al., 2014). We define a recruit to be a juvenile individual that has settled on the reef within the previous year, which also encompasses the size we are first able to sample (3.5-6.0 cm for parentage studies) (Fig. 1). In theory, it does not matter how we define a recruit as long as we use that definition in our calculations of both egg-recruit survival and LEP. In our system, however, while it is straightforward to calculate LEP from any size, we did not have enough tagged recruits to reliably estimate survival to different recruit sizes. Instead, we choose the mean size of offspring matched in the parentage study as our best estimate of the size of a recruit ( $\text{size}_{\text{recruit}}$ ) and tested sensitivity to different recruit sizes by sampling from a uniform distribution over the sizes the recruit stage covers (3.5-6 cm, Table A1).

## **Accounting for density-dependence**

Ideally we would assess persistence metrics when the population is at low abundance and not limited by density-dependence. Clownfish have strong social hierarchies and juveniles on an anemone will prevent others from settling there as well (seen in *A. percula*, Buston, 2003a). Each anemone, therefore, can house only one settling clownfish, with anemones already occupied by *A. clarkii* settlers essentially unavailable as habitat. This density-dependent mortality will artificially reduce the

apparent survival of new recruits, biasing persistence metrics. We account for this density-dependent mortality by multiplying our estimate of settling recruits (the numerator of eqn. 8) by the proportional increase (DD) in unoccupied anemones at our sites if all of the *A. clarkii* anemones were unoccupied, where  $p_A$  is the proportion of anemones occupied by *A. clarkii* and  $p_U$  is the proportion of unoccupied anemones:  $DD = \frac{(p_U + p_A)}{p_U} = 1.71$ . We present results with this density-dependence modification (with subscript DD) in the main text and without in the appendix (Figs. C.2, C.3).

### Estimated abundance over time

We also considered trends in abundance of breeding females at each site over time ( $F_{i,t}$ ) to compare to our replacement-based estimates of persistence. Similarly as for offspring, we scaled up the number of females caught ( $F_c$ ) at each site  $i$  in each sampling year  $t$  by the proportion of habitat sampled in that site and year  $P_{h_{i,t}}$  and by the probability of capturing a fish  $P_c$ :

$$F_{i,t} = \frac{F_{c_{i,t}}}{P_{h_{i,t}} P_c} \quad (9)$$

We fit a mixed effects model to estimate the number of fish in each year as a Poisson variable  $\lambda_a$  with effect  $m_t$  of year  $t$  and with site as a random effect  $m_i$  using the package `lme4` in R (Bates et al., 2015):

$$\begin{aligned} F_{i,0} &\sim Poisson(\lambda_a) \\ F_{i,t} &= (\lambda_a + m_i)m_t t. \end{aligned} \quad (10)$$

We estimate  $\lambda_a$  for an average site as well as the individual sites.

## Results

From the mark-recapture analysis of tagged and genotyped fish, we estimated mean values of  $L_\infty = 10.70$  cm (with 95% confidence intervals 9.81-11.65) and  $K = 0.864$  (0.80-0.91) for the von Bertalanffy growth curve parameters (eqn. 5, Fig. 3b, Table A1). For juvenile and adult (post-recruitment) survival on a log-odds scale, the best-fit model has an effect of site and a positive effect of size (eqn. B.5, Table A1, Figs. 3c, B.3). The accompanying best-fit model for recapture probability has negative effects of size and diver distance from anemone (eqn. B.6, Table A1, Fig. B.4).

For our persistence metrics, we present the estimate using the demographic and connectivity input values without uncertainty (the mean of the uncertainty distributions, with the exception of the size range for recruit), as the best estimate and the range with uncertainty shown in brackets. Using our best estimates for growth, survival, and fecundity, we calculated an average value of LEP across sites of 721 eggs [82, 31657] (Fig. 4b), with best estimates at individual sites ranging from 0 to 1754 eggs. Adult survival has the largest effect on the value of LEP (Fig. C.5), as higher-surviving adults have more opportunities to reproduce and at larger sizes.

We estimated egg-recruit survival  $S_{e_{DD}}$  to be 0.002 [3.5e-05, 0.014] when we correct for density-dependence in our data. Uncertainty in the size of transition to breeding female  $L_f$  has the largest effect on egg-recruit survival (Fig. C.7); the larger the transition size to female, the fewer tagged eggs we estimate were produced by our genotyped parents and the higher our estimate of egg-recruit survival. This differs

from our finding above that adult survival has the largest effect on LEP because the starting size of the individual considered is lower when we estimate LEP for a recruit (4.37 cm, 3.5-6.0cm range) than LEP for a parent (6.0cm). Fish considered parents in our parentage analysis have already survived one or more years since recruiting so the transition to breeding female plays a larger role in the number of eggs they are likely to produce than for fish who have just recruited.

We estimated average lifetime recruit production ( $LRP_{DD}$ ) across sites to be 1.45 [0.62, 7.78] (Fig. 4c), with best estimates of  $LRP_{DD}$  at individual sites ranging from 0 to 3.5. 94% of the estimates of average  $LRP_{DD}$  across sites are one or larger, above the threshold necessary for replacement before considering dispersal. This means that individuals at our sites produce enough surviving offspring before considering dispersal to be able to replace themselves, but LRP does not tell us whether those offspring will settle within our sample sites and drive persistence.

We did not find any sites with a best estimate of  $SP_{DD} \geq 1$  (Fig. 5a), suggesting that none of our sites could persist in isolation. The site Haina ( $SP_{DD} = 0.047$  [9.5e-05, 0.60]) has the largest SP but none of the estimates with uncertainty are  $\geq 1$ . We saw estimates  $> 1$  for Caridad Cemetery but those were due to the high uncertainty in adult survival due to the lack of recaptures at that site and are unlikely to indicate persistence.

Most of the connectivity occurs among the sites in the northern part of our sample area, from Palanas to Caridad Cemetery, and at the southern part of our sample area, from Tomakin Dako to Sitio Baybayon (Fig. 5b), where the sites tend to be the largest, have higher abundances, and have higher survivals (though not

entirely). Sites at the edges of our sampling region seem to be the strongest sub-populations, which means many of the recruits they produce could be exported away from our sites rather than into our sampling region.

For network persistence, our best estimate of the dominant eigenvalue of the realized connectivity matrix  $\lambda_{c_{DD}}$  is 0.15 [0.064, 1.54], with  $p(\lambda_{c_{DD}} \geq 1) = 0.005$  when we correct for density-dependence in the data (Fig. 5c). Network persistence for our sites is unlikely but not impossible. Our estimate of local replacement ( $LR_{DD}$ ) was 0.16 [0.07, 0.88] when correcting for density-dependence in the data, also suggesting lack of independent persistence of our group of sites and very similar to our  $\lambda_{c_{DD}}$  estimate. When we calculated LR using all arriving recruits to our sites, however, rather than just those originating there, our best estimate was  $> 1$  (2.08 with 99.8% estimates  $\geq 1$ ), suggesting that there is recruit-recruit replacement at our sites when we include immigrants. While both  $LR_{DD}$  and  $\lambda_{c_{DD}}$  tell us about the ability of our sites to persist as an isolated group, they differ in their assumption of the structure of the population.  $LR_{DD}$  gives us the number of recruits individuals at our sites produce that settle within our sites, assuming the network of sites is a single well-mixed unit, while  $\lambda_{c_{DD}}$  accounts for the spatial structure and multi-generation dynamics.

Based on our estimates of  $LRP_{DD}$ ,  $LR_{DD}$ , and  $\lambda_{c_{DD}}$ , it is possible but unlikely that our set of sites is able to persist in isolation as a closed system. With our existing site configuration and dispersal kernel estimate, we would need a value of LRP of 8.84 (an egg-recruit survival of 0.012 with our estimated value of LEP or a value of LEP of 4406 with our estimated value of  $S_{e_{DD}}$ ) to have a best estimate of  $\lambda_{c_{DD}} = 1$  and network persistence. Retaining essentially all recruits produced from our sites

would enable our set of sites to persist, given that LRP is very likely  $\geq 1$ . With our estimated dispersal kernel, however, increasing the amount of habitat in our region (currently about 20%) even to 100% gives a best estimate  $\lambda_{c_{DD}} = 0.95$ , with 59% of the estimates with uncertainty  $\geq 1$  (Fig. 6), suggesting isolated persistence of the region would be possible but not certain.

Our estimated abundance of females over time has a slight positive trend for the average site ( $m_t = 1.08$ , Fig. 4a), suggesting a slight increase in population size for the population overall through time. Most individual sites also show a slight positive trend in female abundance through time, though one large site shows declines (Fig. 4a, Fig. C.1s).

## Discussion

In this first assessment of demographic persistence of a coastal marine metapopulation, we did not find strong evidence for either self-persistence of an individual patch or network persistence of the entire system as an isolated region. Network persistence of the group of sites is possible at the upper end of our estimates with uncertainty but unlikely (0.5% of estimates). This inability to persist as an isolated region does not necessarily mean that the populations at our sites are declining, however. Our assessments of population trends - both abundance over time and replacement of recruits when we include immigrants - find that the population levels at our sites are stable or increasing slightly. Taken together, our metrics suggest that the sites in our region have stable populations on average but require input of immigrants to persist. The portion of coastline we sampled is likely a sink region of a larger

metapopulation, given that there does not seem to be a long-term decline in the population.

For our sites to persist as an isolated network, either the number of surviving recruits produced by an average recruit (LRP) would need to be higher or more recruits would need to be retained within the region. To see a best estimate of network persistence with our existing site configuration and estimated connectivity, LRP would be about six times higher than our best estimate, about 13% higher than the top end of our estimate range. This higher LRP value is similar to estimates of lifetime reproductive success that include dispersal to the natal reef in *A. percula* in Kimbe Bay (Salles et al., 2020), however, suggesting it is not an unreasonable level of production for clownfish. Habitat quality affects production in other clownfish systems (e.g., Salles et al., 2020; Hayashi et al., 2019), and our sites likely have generally low reef health due to anthropogenic effects such as pollution and silt from a nearby gravel mine. Adult survival, for example, was lower at the two sites just downstream of the gravel mine (N. and S. Magbangon in Fig. B.3). Alternately, higher connectivity and retention of offspring among our sites could lead to network persistence. Though lack of sufficient connectivity and retention is thought to inhibit network persistence in other systems (e.g., a collection of reserves for eastern oysters (*Crassostrea virginica*) in the Pamlico Sound in North Carolina; Puckett and Eggleston, 2016), low production of surviving recruits due to poor habitat quality seems the more likely explanation in our system. Our dispersal kernel is comparable to those estimated for other species of reef fish, both similar in shape (e.g., Harrison et al., 2012; DAloia et al., 2015) and with a mean dispersal distance of a similar

range to that estimated for *A. percula* in Kimbe Bay (13.3 and 18.9 km compared to our estimate of 8.2 km; Almany et al., 2017), which has been found to be persistent without input from outside reefs (Salles et al., 2015).

We do not find clear evidence for network persistence for our sites despite estimates of the mean dispersal distance of *A. clarkii* from previous genetic work (11 km, Pinsky et al., 2010) and from our samples (8.2 km, Catalano et al., in prep) that are well within the 30 km span of our sites. Though the length of our sampling region is more than twice the mean dispersal distance, usually sufficient for persistence of a population in an isolated reserve (e.g., Lockwood et al., 2002), our sampling region contains only about 20% habitat, rather than a continuous stretch, which may be too low of habitat coverage to support network persistence, with sites too small to show self-persistence. Habitat in our region has likely been declining in recent decades. The region was hit in 2013 by Typhoon Haiyan, one of the strongest typhoons ever to make landfall, which destroyed reef habitat, including one of our northern sampling sites, and fishers noticed prior habitat changes when asked in the early 2000s (Jennifer Selgreth, unpublished data). Our sensitivity test to proportion habitat suggests that even 100% habitat in our sampling region does not give a best estimate with network persistence, however, though 50% of our estimates show persistence ( $\lambda_{C_{DD}} \geq 1$ ) at about 90% habitat. For self-persistence, our individual sites are likely too small: the largest site, Haina, is only about 0.8km wide, about 10 times smaller than the mean dispersal distance. This is in contrast to the findings on reefs surrounding the isolated Kimbe Island, however, where several *A. percula* subpopulations in lagoons of similar size as our sites were found self-persistent (Salles et al.,

2015). The suggestion of a habitat shortage in our sampling region is partially dependent on our assumption that larvae land in non-habitat between patches and die. Larvae have some navigational and habitat-finding capabilities (e.g. Elliott et al., 1995; Fisher, 2005), so we could be underestimating their ability to find habitat in our calculations, which would decrease the amount of habitat required for network persistence.

We suggest that our region is a sink area of a larger metapopulation but the area required for the larger persistent metapopulation depends on the production and connectivity of outside patches. If surrounding patch populations have a similar LRP and level of connectivity as our sites, increasing the area of the network to include them also would not achieve network persistence. If nearby sites have higher egg production or egg-recruit survival, however, it might not take much of an increase in area considered to create a persistent network. Nearby reef sites such as Cuatro Islas, for example, with higher coral cover and less silt, could have higher survival of fish and be contributing recruits to our sites.

An alternative to our sampled sites as a sink portion of a larger metapopulation is that variability in demography or dispersal on a longer scale than our sampling time could lead to persistence. For example, rockfish on the west coast of the United States have highly variable and episodic recruitment, where successful recruitment events occur on the decadal scale and sustain the population until the next strong recruitment event (e.g., Tolimieri and Levin, 2005). Though perhaps not as extreme as in the California Current system, ocean connectivity is still variable in the Coral Triangle region surrounding our study sites, with estimates suggesting that 20 year

simulations are necessary to capture the full extent (Thompson et al., 2018). Our study, though relatively long term, could have missed a particularly strong recruitment event that would enable local persistence of the set of populations we sampled.

Though we estimate abundance trends and do not find overall declines, it is possible we could have missed declines due to our sampling design. Our sampling study was designed for mark-recapture analyses rather than a comprehensive habitat or abundance estimate so we did not sample all areas of all sites each year. We scaled up the number of fish we caught to account for those we missed using the proportion of tagged anemones we visited, which assumes that all tagged anemones are equally likely to be sampled. In reality, tags that no longer have anemones next to them are likely harder to find and sample. If anemones are disappearing over time at our sites, we might be overestimating the number of fish present and missing population declines at our sites that would mean lack of persistence even with outside input.

Including uncertainty in our empirical estimates of demographic and dispersal parameters allows us to better understand how likely it is that the population is persistent and which processes contribute the most uncertainty. We see a wide range of estimated metric values, spanning of network persistence for our set of sites to far from it. In our study, demographic parameters, particularly adult survival, have a large effect on whether or not we think the population is persistent. Other metapopulation studies also find higher sensitivity to demographic rather than connectivity parameters (e.g., on source or sink status in bicolor damselfish; Figueira, 2009), including particular sensitivity to adult survival (on metapopulation growth rate in mussels; Carson et al., 2011). Our estimates of connectivity are simpler than our

estimates of demography, with no spatial variability (which can be important in understanding demographic connectivity; Johnson et al., 2018), and a more thorough assessment could alter their relative effect on persistence, but this suggests that sufficient offspring production and survival has a larger effect on persistence at these relatively small scales of connectivity. Uncertainty in our sampling, particularly how likely we are to capture a fish, however, contributes the most uncertainty to whether we determine the population to be persistent, highlighting the challenge of estimating these metrics empirically. For a marine metapopulation, our system is relatively uncomplicated; as we accumulate more empirical assessments of metapopulations to compare to our expectations from theory and models, we will have to think carefully about how to handle uncertainty as we move to tackling larger and more complicated systems.

Persistence criteria, such as those detailed in Hastings and Botsford (2006) and Burgess et al. (2014), ask whether a population at low abundance can grow and recover rather than going extinct. Density-dependence is often ignored at low abundances (Botsford et al., 2019) so is not explicitly considered in persistence metrics. In real populations, however, it can be challenging to estimate density-independent demographic rates, as density-dependence is occurring in the population as it is sampled. In *A. clarkii*, density-dependence is likely most important immediately post-settlement, as for many fish species, but is also relatively easy to measure at that point and accounted for in our analyses. Density-dependence could continue to be important throughout the life history, however, due to the social hierarchies in colonies of clownfish (e.g. Buston and Elith, 2011). In other species of clownfish,

individuals on the same anemone maintain strict size spacing, restricting their food intake and growth to avoid encroaching on the position of another fish and being attacked or evicted (seen in *A. percula*, Buston, 2003a,b). This suggests that while fish are in the pre-reproductive queue, density-dependence may lower growth rates compared to the growth of fish alone on an anemone, as would be the case in a population at low abundance. We include the primary effect of density-dependence on our estimate of egg-recruit survival but other estimates, particularly growth and survival, would also likely be higher in the absence of density-dependence and increase LRP.

Understanding persistence is critical for the management of spatial populations, such as siting marine protected areas (e.g., Kaplan et al., 2009), assessing habitat fragmentation risks (e.g., Smith and Hellmann, 2002; Fahrig, 2001) and conserving species in the face of climate change (e.g., Coleman et al., 2017; Fuller et al., 2015). Though models and theory provide us with expectations, we are only recently beginning to be able to tackle these questions of persistence empirically in model systems such as clownfish and other sedentary tropical reef fish (e.g., Salles et al., 2015; Johnson et al., 2018). With parentage analyses now being extended to temperate species (e.g., Baetscher et al., 2019) and a better understanding of how biophysical models compare to larval dispersal patterns (Bode et al., 2019) we are beginning to move beyond model species and investigate persistence in harvested and spatially-managed systems (e.g., Garavelli et al., 2018). Our study shows the importance of long term sampling and careful consideration of the different demographic processes that affect our metric calculations, such as density-dependence and sampling biases,

to distinguish persistence ability from population trajectories and understand marine population dynamics in empirical systems.

## Figures

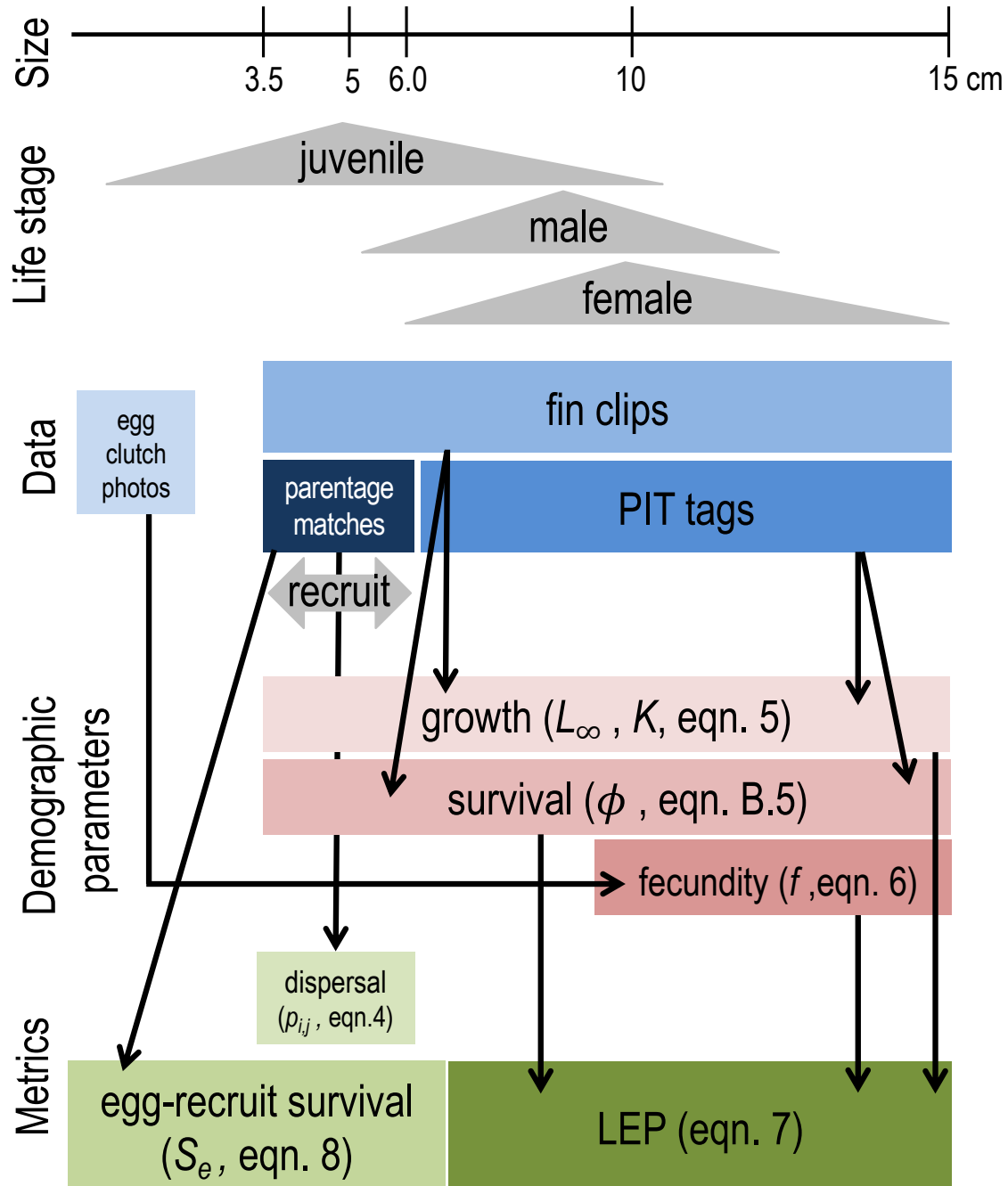


Figure 1: The data collected for fish at each life stage and how they match to the equations and metrics estimated. We consider recruits to be offspring in their first year of settlement, represented by the 3.5-6.0 cm range.

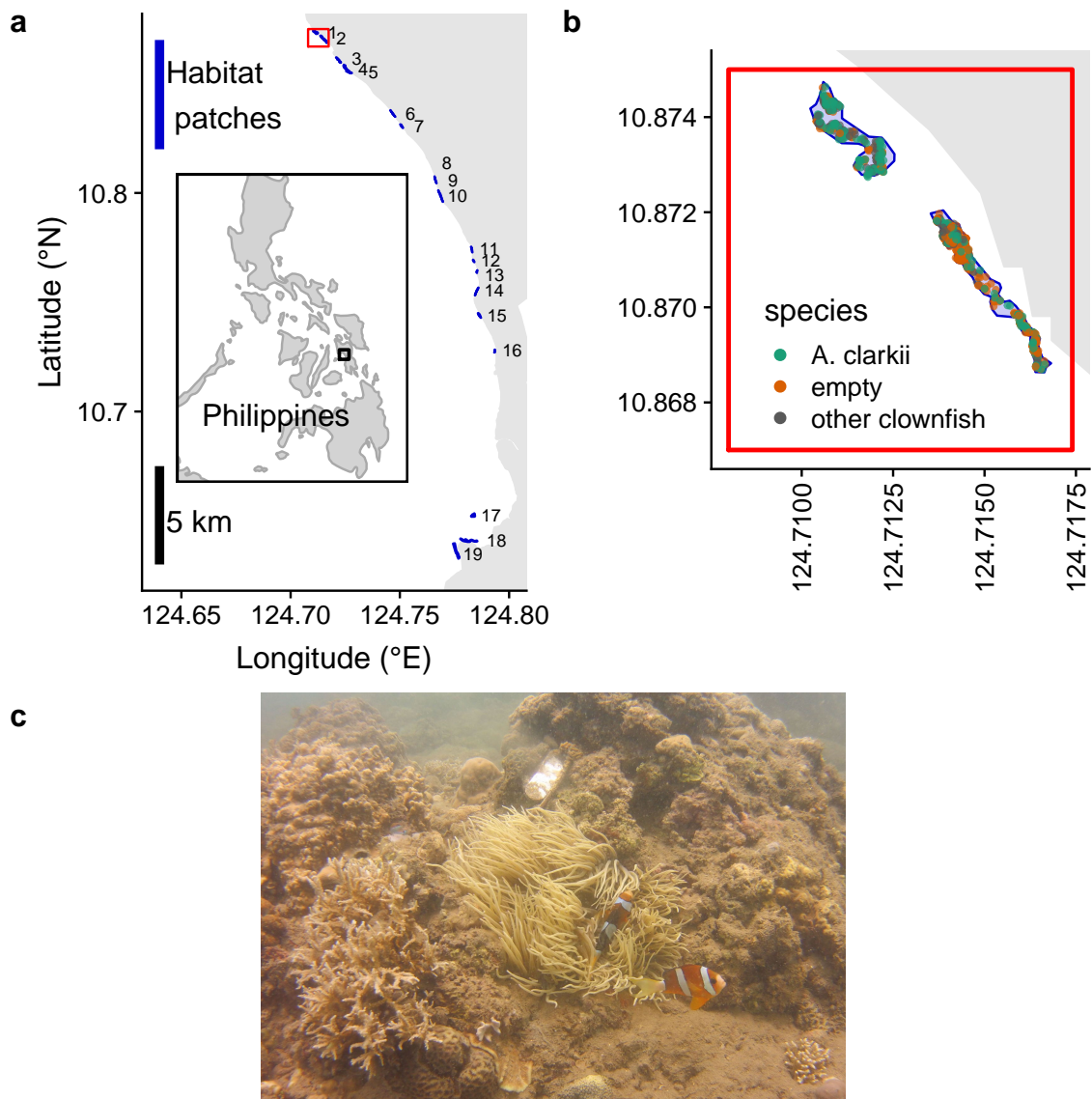


Figure 2: a) Map of the sites along the coast of Leyte in the Philippines. From north to south, the patches are: 1) Palanas, 2) Wangag, 3), North Magbangon, 4) South Magbangon, 5) Cabatoan, 6) Caridad Cemetery, 7) Caridad Proper, 8) Hicop South, 9) Sitio Tugas, 10) Elementary School, 11) Sitio Lonas, 12) San Agustin, 13) Poroc San Flower, 14) Poroc Rose, 15) Visca, 16) Gabas, 17) Tomakin Dako, 18) Haina, and 19) Sitio Baybayon. b) Zoomed-in map of the two northern-most sites, Palanas and Wangag, to show anemone arrangement with anemones colored as occupied by *A. clarkii* (green), occupied by other clownfish species (orange), or unoccupied by clownfish (grey). c) An example anemone occupied by *A. clarkii* in a typical habitat at the sites. The metal anemone tag is visible just above the anemone on the rock.

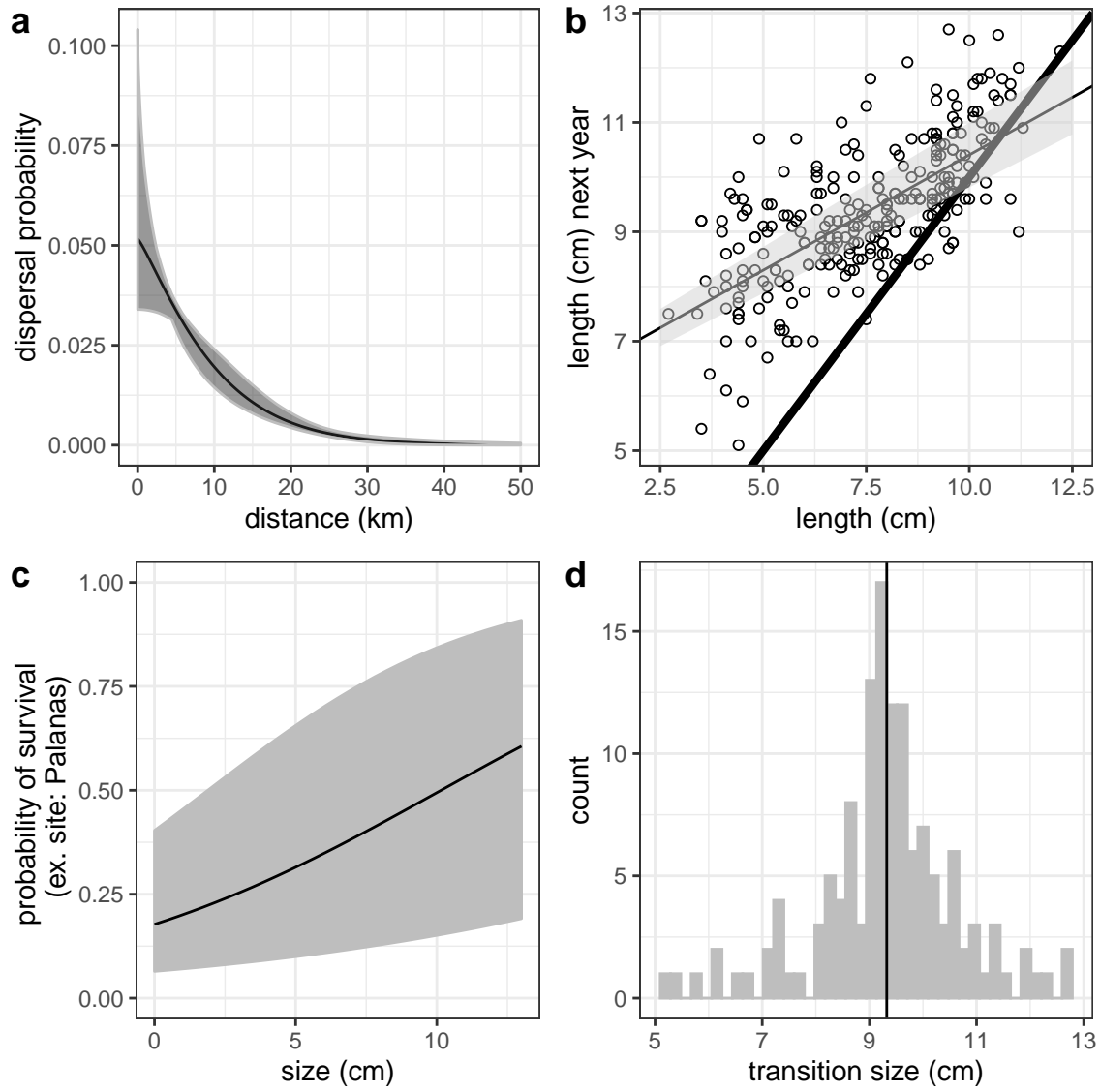


Figure 3: Best estimates (solid black line) and uncertainty (grey) for dispersal (a), growth, including the 1:1 line in thick black (b), post-recruit annual survival at Palanas as an example site (c), and size at female transition (d) parameters. Best est

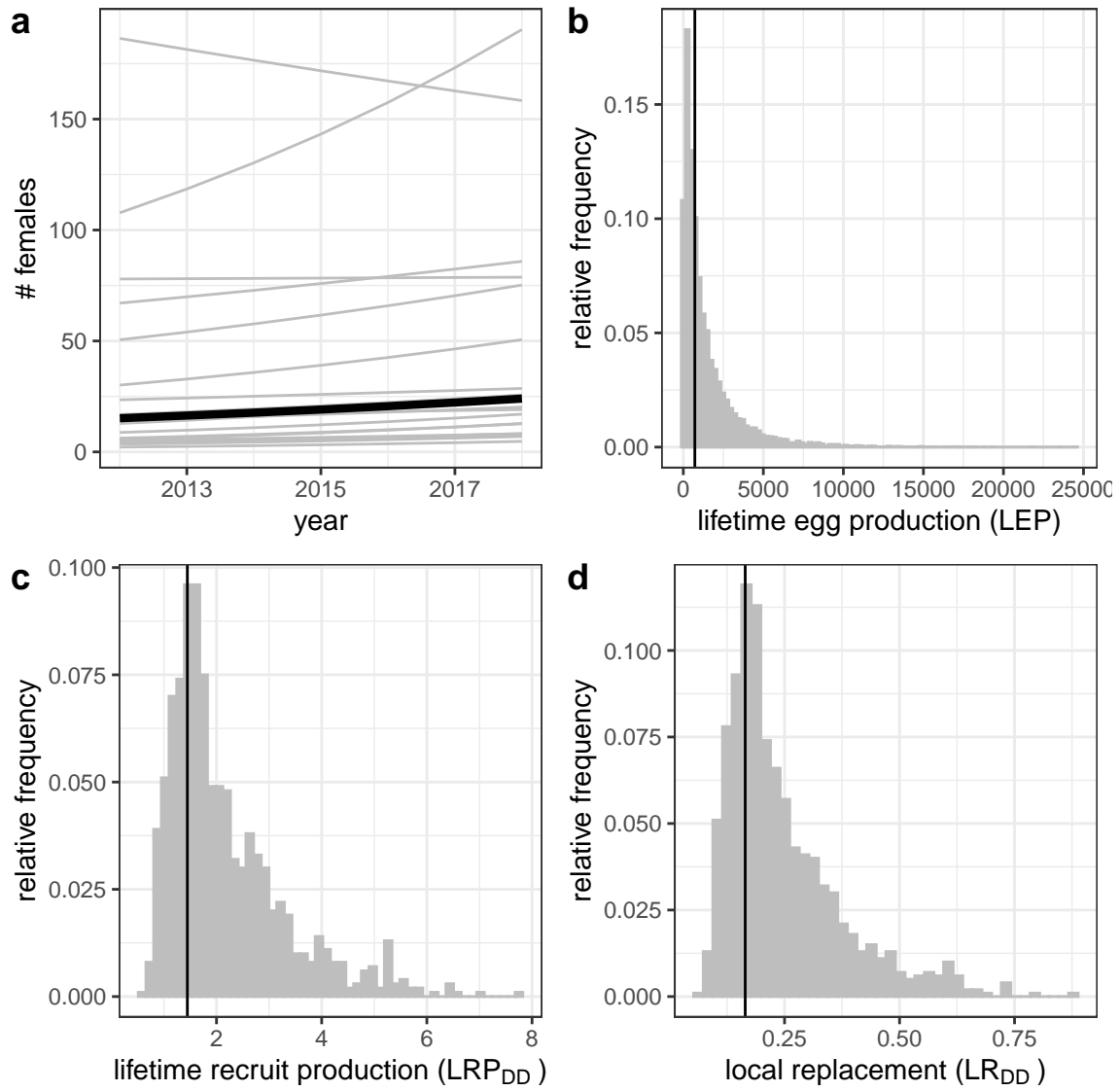


Figure 4: Estimates of a) estimated abundance of females over time at each individual site (grey lines) and for an average site (black line), b) individual-site LEP for all sites with the best estimate averaged across sites (black line), c) average  $LR_{DD}$  across sites, and d) local replacement, showing the best estimate (black solid line) and range of estimates considering uncertainty in the inputs (grey). Estimates of LRP and local replacement include compensation for density-dependent mortality in early life stages.

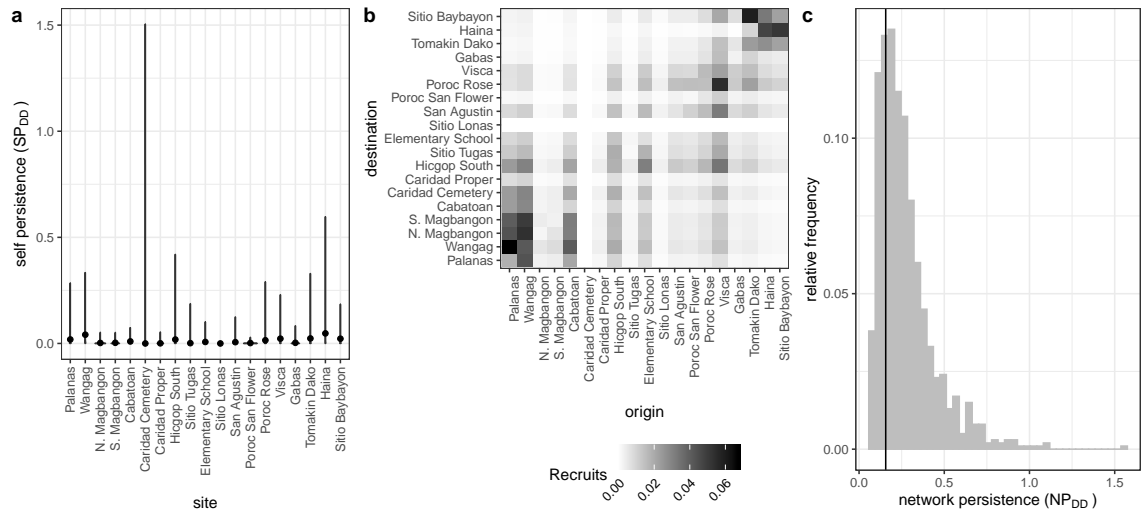


Figure 5: Values of self-persistence (a), realized connectivity among sites (b), and network persistence (c). All estimates include compensation for density-dependence in early life stages. For self-persistence (a) and network persistence (c), the best estimate is shown with in black (point for (a), line for (c)) and the range of estimates considering uncertainty is shown in grey.

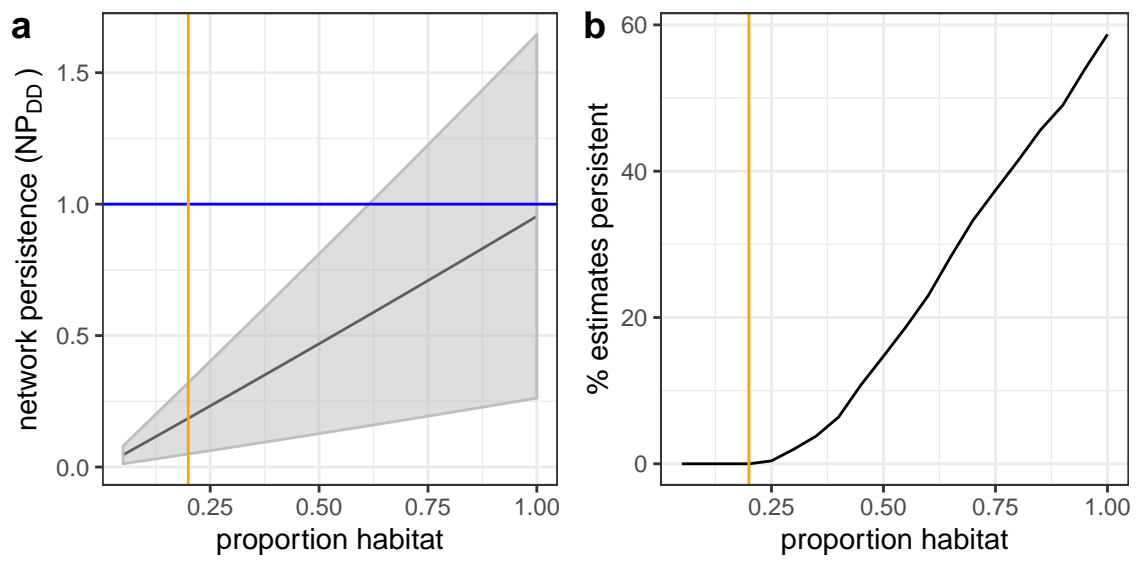


Figure 6: Sensitivity of network persistence to the proportion of the sampling region that is habitat. (a) The best estimate of  $\lambda_{cDD}$  with the standard deviation of the estimates with uncertainty for 19 patches of equal size and spacing with adult survivals for an average patch. (b) The percentage of estimates from the runs in (a) with  $\lambda_{cDD} \geq 1$  with increasing proportion habitat.

# Appendix

## A Summary of parameters

Parameter	Description	Best estimate	Range in uncertainty runs	Notes
$k_d$	scale parameter in dispersal kernel	-2.33	-2.81 to -1.22	eqn. 4, estimated using methods in Bode et al. (2018) in Catalano et al. (in prep)
$\theta$	shape parameter in dispersal kernel	1.19	0.63 to 2.04	eqn. 4, estimated using methods in Bode et al. (2018) in Catalano et al. (in prep)
$L_\infty$	average asymptotic size (cm) in von Bertalanffy growth curve	10.70 cm	9.81 to 11.65 cm	eqn. 5
$K$	growth coefficient in von Bertalanffy growth curve	0.864	0.80 to 0.91	eqn. 5

$b_{\phi_{Cabatoan}}$	intercept for adult survival at 0 cm at Cabatoan	-1.78	$\pm 0.33$ standard error	on a log-odds scale, eqn. B.5
$i_{\phi_{Cardidad Cemetery}}$	addition to intercept for survival at Caridad Cemetery	-19.61	$\pm 2994$ standard error	on a log-odds scale, eqn. B.5
$i_{\phi_{Elementary School}}$	addition to intercept for survival at Elementary School	-0.11	$\pm 0.41$ standard error	on a log-odds scale, eqn. B.5
$i_{\phi_{Gabas}}$	addition to intercept for survival at Gabas	-0.42	$\pm 0.58$ standard error	on a log-odds scale, eqn. B.5
$i_{\phi_{Haina}}$	addition to intercept for survival at Haina	0.12	$\pm 0.35$ standard error	on a log-odds scale, eqn. B.5
$i_{\phi_{Hicgop South}}$	addition to intercept for survival at Hicgop South	-0.06	$\pm 0.46$ standard error	on a log-odds scale, eqn. B.5

$i_{\phi_{N.Magbangon}}$	addition to intercept for survival at N. Magbangon	-1.31	$\pm$ 0.38 standard error	on a log-odds scale, eqn. B.5
$i_{\phi_{Palanas}}$	addition to intercept for survival at Palanas	0.24	$\pm$ 0.26 standard error	on a log-odds scale, eqn. B.5
$i_{\phi_{PorocRose}}$	addition to intercept for survival at Poroc Rose	-0.19	$\pm$ 0.44 standard error	on a log-odds scale, eqn. B.5
$i_{\phi_{PorocSanFlower}}$	addition to intercept for survival at Poroc San Flower	-0.52	$\pm$ 0.48 standard error	on a log-odds scale, eqn. B.5
$i_{\phi_{SanAgustin}}$	addition to intercept for survival at San Agustin	-0.47	$\pm$ 0.50 standard error	on a log-odds scale, eqn. B.5
$i_{\phi_{SitioBaybayon}}$	addition to intercept for survival at Sitio Baybayon	0.02	$\pm$ 0.26 standard error	on a log-odds scale, eqn. B.5

$i_{\phi_{S.Magbangon}}$	addition to intercept for survival at S. Magbangon	-1.08	$\pm$ 0.48 standard error	on a log-odds scale, eqn. B.5
$i_{\phi_{TomakinDako}}$	addition to intercept for survival at Tomakin Dako	0.39	$\pm$ 0.33 standard error	on a log-odds scale, eqn. B.5
$i_{\phi_{Visca}}$	addition to intercept for survival at Visca	0.33	$\pm$ 0.35 standard error	on a log-odds scale, eqn. B.5
$i_{\phi_{Wangag}}$	addition to intercept for survival at Wangag	0.35	$\pm$ 0.25 standard error	on a log-odds scale, eqn. B.5
$b_a$	size effect for adult survival	0.15	$\pm$ 0.03 standard error	on a log-odds scale, eqn. B.5
$\beta_e$	coefficient for eyed eggs	-0.608		eqn. 6, Yawdoszyn et al. (in prep)
$\beta_l$	size effect in eggs-per-clutch relationship	2.39		eqn. 6, Yawdoszyn et al. (in prep)

$b$	intercept in eggs-per-clutch relationship at female size 0 cm	1.17		eqn. 6, Yawdoszyn et al. (in prep)
$c_e$	egg clutches per year	11.9		eqn. 6, Holtswarth et al. (2017)
$\text{size}_{\text{recruit}}$	size (cm) of recruited offspring	mean of size of offspring in parentage analysis = 4.37 cm	3.5 - 6.0 cm	drawn from uniform distribution across range
$\text{size}_{\text{recruit},sd}$	standard deviation of size of a recruit	0.1		used in discretization of IPM for LEP
$\text{size}_{sd}$	standard deviation distribution of sizes of a fish in the next year	1.45		used in discretization of IPM for LEP, estimated from range of sizes for fish starting at 7.4-7.6 cm and recaptured a year later

$L_s$	minimum size in LEP IPM	0 cm		eqn. 7
$U_s$	maximum size in LEP IPM	15 cm		eqn. 7
$L_f$	size at transition to female	9.32 cm	5.2 - 12.7 cm	drawn from distribu- tion in data
$R_m$	number of off- spring matched to parents	62 offspring		eqn. 8
$N_g$	number of geno- typed parents	1719 fish		eqn. 8
$P_h$	proportion of sites sampled cumulatively across time	0.41		eqn. 8, details in B.1
$P_d$	proportion of dispersal kernel area from each site covered by our sampling region	0.57		eqn. 8, details in B.3.0.1

$P_c$	probability of capturing a fish	0.56	drawn from beta distribution with parameters $\alpha_{P_c} = 1.44$ and $\beta_{P_c} = 1.13$	eqn. 8, details in B.2
$P_s$	proportion of our sampling region that is habitat	0.20		eqn. 8, details in B.3.0.2
DD	proportion of habitat that would be available without density-dependence at settlement	1.71		eqn. 8
$p_U$	proportion of anemones unoccupied by clownfish	0.53		used to estimate DD

$p_A$	proportion of anemones oc- cupied by $A$ . <i>clarkii</i>	0.38		used to estimate DD
-------	--	------	--	---------------------

Table A1: Summary of parameter symbols, definitions, and values.

## B Method details

### B.1 Proportion of habitat sampled

We used tagged anemones to estimate the proportion of habitat sampled at each site in each year ( $P_{h_{i,t}}$ ). We tagged each anemone that is home to *A. clarkii*, with a metal tag, which is relatively permanent and easy to re-sight (the anemone tag is visible above the anemone in Fig. 2c), so we consider the total number of metal tags at each site to be the total number of anemones that are habitat. We divide the number of tagged anemones visited each sampling year by the total number of metal tags at that site to get the proportion of habitat sampled. We use proportion of anemones rather than proportion of total site area because anemones, and therefore habitat quality, are unevenly distributed across the site; areas we did not visit are likely to have a lower density of anemones than the areas we did sample.

For scaling the number of tagged recruited offspring to account for areas of our sites we did not sample, we use the overall proportion habitat sampled across all sites and sampling years ( $P_h$ ). We sum the metal-tagged anemones we visited across all sites and years to get the total number of metal-tagged anemones we visited while sampling. We then divide that by the number of anemones we could have sampled, the sum of total metal-tagged anemones across all sites multiplied by the number of sampling years, to get the overall proportion habitat sampled across our sites and sampling years.

Table A2: Table showing the percent of anemones surveyed at each site, ordered from north to south, in each sampling year.

Site	# Total anems	% Habitat surveyed						
		2012	2013	2014	2015	2016	2017	2018
Palanas	137	29	58	47	63	85	86	86
Wangag	296	18	32	42	34	26	49	68
N. Magbangon	105	5	12	40	63	63	0	5
S. Magbangon	34	41	56	32	0	65	0	71
Cabatoan	26	42	58	58	65	73	0	62
Caridad Cemetery	4	0	75	50	0	50	50	50
Hicgop South	18	0	67	22	28	56	83	78
Elementary School	8	0	100	38	88	88	88	100
San Agustin	17	94	65	71	65	100	82	76
Poroc San Flower	11	100	82	73	73	55	82	64
Poroc Rose	13	100	100	69	31	23	69	69
Visca	13	100	100	23	38	62	85	62
Gabas	9	0	0	0	44	44	67	0
Tomakin Dako	50	0	24	22	36	34	60	68
Haina	104	0	6	13	13	10	56	80
Sitio Baybaon	260	0	14	30	33	30	41	80
Overall	1105	16	31	37	39	42	48	68

## B.2 Probability of capturing a fish, from recapture dives

We use mark-recapture data from recapture dives done within a sampling season to estimate the probability of capturing a fish. During some of the sampling years, portions of the sites were sampled again within a few weeks of the original sampling dives. We assume there is no mortality of tagged fish between the original sampling dives and the recapture dives because they are so close in time and that fish do not change their behavior or response to divers, so therefore assume that the probability of recapturing a fish is the same as the probability of capturing a fish on a sampling dive. For each recapture dive, we use GPS tracks of the divers to identify the anemones covered in the recapture dive and the set of PIT-tagged fish encountered on those anemones during the original sampling dives. We estimate the probability of capture  $P_c$  as the number of tagged fish caught during the capture dive  $m_2$  divided by the total number of fish caught on the recapture dive  $n_2$ :  $P_c = \frac{m_2}{n_2}$ . The value of  $P_c$  from each recapture dive is reported in Table A3.

We use the mean  $P_c$  across all 14 recapture dives, covering XX sites in 3 sampling seasons (2016, 2017, 2018), as our best estimate. Because there are so few recapture dives compared to the number of times we calculate the metrics to show the range of uncertainty, we represent the probability of capture as a distribution, rather than sampling directly from the values calculated for each recapture dive. The distribution of capture probabilities across the 14 dives is quite skewed so we represent it as a beta distribution, using the mean  $\mu_{P_c}$  and variance  $V_{P_c}$  of the set of 14 values to find the appropriate  $\alpha_{P_c}$  and  $\beta_{P_c}$  parameters, where

$$\alpha_{P_c} = \left( \frac{1 - \mu_{P_c}}{V_{P_c}} - \frac{1}{\mu_{P_c}} \right) \mu_{P_c}^2 \quad (\text{B.1})$$

$$\beta_{P_c} = \alpha_{\mu_{P_c}} \times \frac{1}{\mu_{P_c} - 1}. \quad (\text{B.2})$$

The mean of the individual capture probability values is  $\mu_{P_c} = 0.56$ , with variance  $V_{P_c} = 0.069$ , which gives beta distribution parameters  $\alpha_{P_c} = 1.44$  and  $\beta_{P_c} = 1.13$ . We sample 1000 values from the beta distribution, then truncate the sample to only values larger than the lowest value of  $P_c$  estimated in an individual dive (0.20), to avoid extremely low values that are sometimes randomly sampled from the distribution but are unrealistically low. We then sample with replacement from the truncated set to get a vector of values the length of the number of runs.

*Talk to Katrina to fill out table with data that went into recapture calcs*

Table A3: Table showing the site, year, number of fish caught on sample dives on the anemones resampled during the recapture dive ( $m_2$ ), number of fish caught on the recapture dive ( $n_2$ ) for each recapture dive.

Site	Year	$m_2$	$n_2$	$P_c$
				0.56
				0.26
				0.89
				0.67
				0.20
				0.83
				0.47
				0.20
				0.83
				1.0
				0.33
				0.58
				0.63
				0.41

### B.3 Scaling up recruits

To estimate the total number of offspring produced by our genotyped parents that survive to recruitment, we scale up the number of matched offspring caught during sampling ( $R_m$ ) to account for recruits we could have missed (Fig. B.1). We scale up by 1) the cumulative proportion of habitat we sampled at our sites over time ( $P_h$ ) to account for recruits at anemones we did not sample (details in B.1), 2) the probability of capturing a fish if we sampled its anemone ( $P_c$ ) to account for fish that escaped during sampling (details in B.2), 3) the proportion of the dispersal kernel from our sites within of our sampling region ( $P_d$ ) to account for fish that dispersed outside of our sampling area (details in B.3.0.1), and 4) the proportion habitat in our

sampling region ( $P_s$ ) to avoid counting mortality of fish dispersing to non-habitat within our region twice (in both the estimate of total recruits and in the integrated dispersal kernel) (details in B.3.0.2), and 5) the proportion of anemones occupied by *A. clarkii* (DD) to account for density-dependent mortality of settling recruits.

### How could we have missed potential recruits originating from our sites?

- 1) Failed to catch recruit when sampling ( $P_c$ )
- 2) Missed sampling some habitat areas within our sites ( $P_h$ )
- 3) Recruit dispersed outside our study region ( $P_d$ )
- 4) Recruit dispersed to non-habitat within our region ( $P_s$ )
- 5) Recruit died due to density-dependent competition with other settlers (DD)

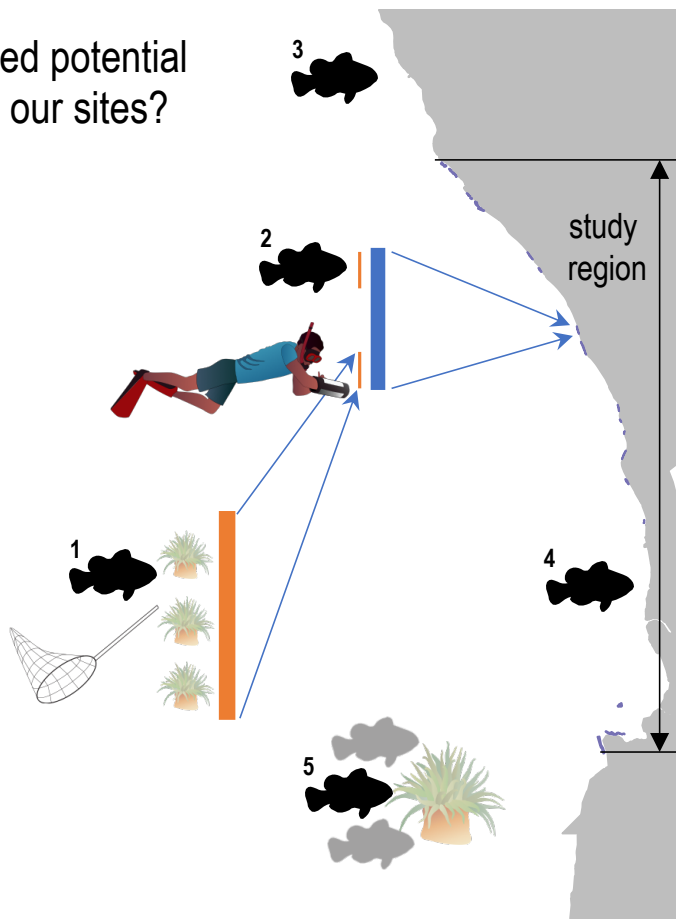


Figure B.1: Schematic of five ways we could have missed recruits while sampling and used to scale up our raw estimate of recruits from matched offspring.

### B.3.0.1 Proportion of dispersal kernel area sampled

To account for recruits that dispersed outside our sampling region, we find the proportion of the dispersal kernels from all parents that falls within our sampling region. For each of the nineteen sites, we find the area ( $A_i$ ) under the kernel from the center of the site to the north edge of the sampling area ( $d_N$ ) (northern-most tagged anemone at Palanas, the northern-most site) and the center of the site to the south edge of the sampling area ( $d_S$ ) (southern-most tagged anemone at Sitio Baybayon, the southern-most site), then multiply by the number of genotyped parents at that site ( $N_{g_i}$ ). We add the total areas together, then divide by the sum of the total area under the dispersal kernel in both directions (1 when kernel is normalized to 0.5) multiplied by the total number of genotyped parents ( $N_g$ ) to get the proportion of the total dispersal kernel area covered by our sampling region ( $P_d$ ):

$$A_i(d) = N_{g_i} \int_0^{d_N} z e^{-(zd)^{\theta}} dd, \quad (\text{B.3})$$

$$P_d = \frac{\sum_{i=1}^{19} A_i}{N_g}. \quad (\text{B.4})$$

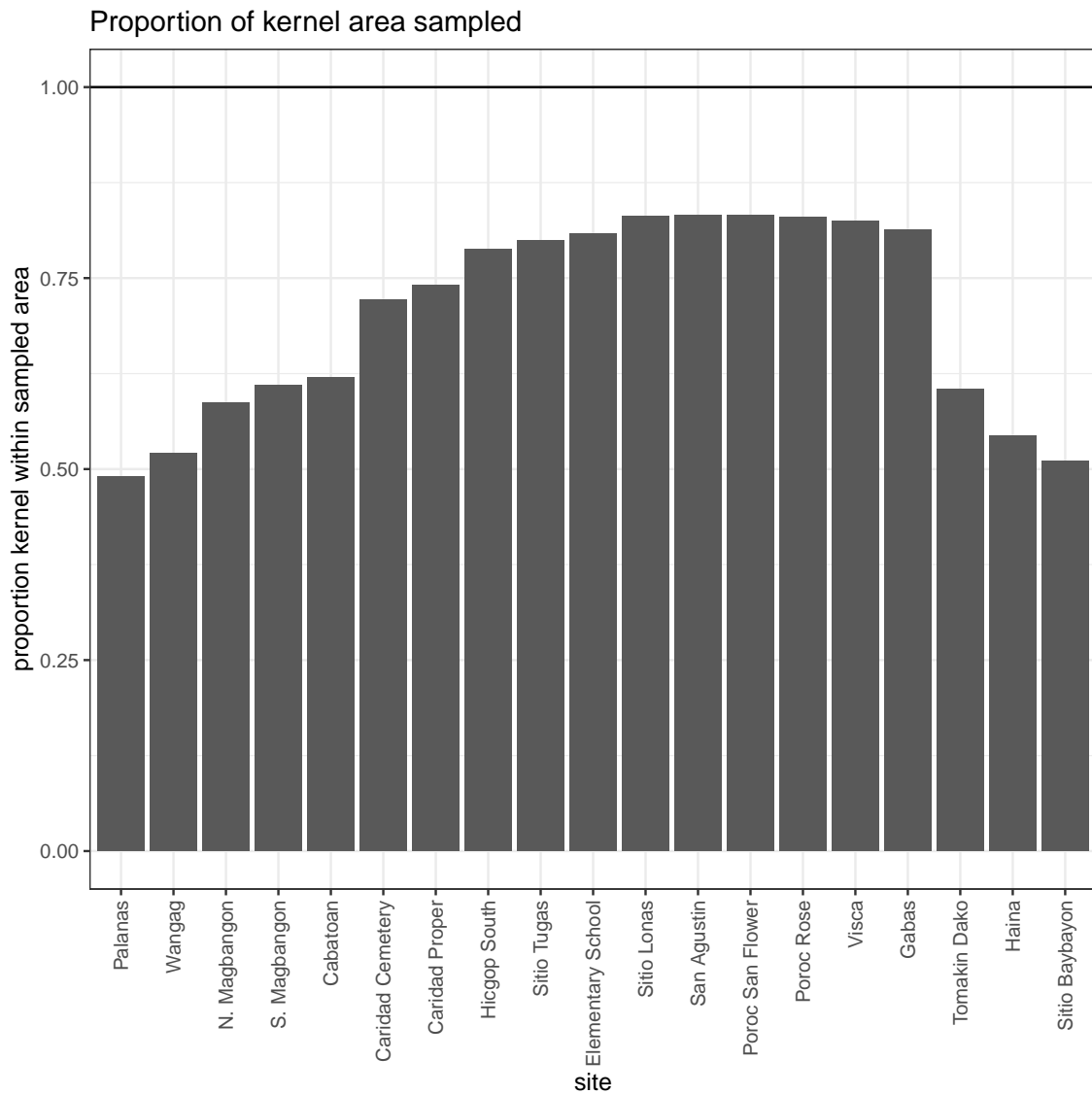


Figure B.2: Proportion of the dispersal kernel area from the center of each site covered by our sampling. Our overall proportion is weighted by the number of parents at each site.

### B.3.0.2 Proportion habitat in sampling area

We assume that larvae are unable to navigate to habitat if they attempt to settle on an unsuitable patch, though clownfish larvae do likely have some ability both to sense good settlement areas, either by detecting host anemones (Elliott et al., 1995; Arvedlund et al., 1999) or conspecifics (e.g. Lecchini et al., 2005, for coral reef fish more broadly), and swim in particular direction (e.g. Bellwood and Fisher, 2001; Fisher, 2005). To avoid counting mortality due to settling on non-habitat twice - once in scaling up our matched recruits, which only includes those who settled on habitat, and once in integrating the dispersal kernel, we scale our estimate of total surviving recruits from our patches by the proportion of our sampling region that is habitat ( $P_s$ ). We find  $P_s$  by summing the lengths of all of our sites, which run approximately north-south, and dividing that by the total distance north-south of our sampling region, giving  $P_s = 0.20$ .

## B.4 Full set of MARK models

We consider the following set of models in MARK for survival ( $\phi$ ) and recapture ( $p$ ) probability, including effects of size ( $S$ ), minimum distance from diver to anemone during surveys ( $D$ ), time ( $t$ ), and site ( $i$ ) (Table A4):

Table A4: Table showing MARK models considered and their relative AICc scores.

Model	Model description	AICc	dAICc
$\phi \sim S + i, p \sim S + D$	survival size+site, recapture size+distance	3104.1	0
$\phi \sim i, p \sim D$	survival site, recapture size+distance	3127.1	23
$\phi \sim i, p \sim D$	survival site, recapture distance	3127.2	23
$\phi \sim S, p \sim S + D$	survival size, recapture size+distance	3139.9	35.8
$\phi \sim S, p$	survival size, recapture distance	3141.6	37.5
$\phi, p \sim S + D$	survival constant, recapture size+distance	3168.3	64.2
$\phi, p \sim D$	survival constant, recapture distance	3169.3	65.2
$\phi \sim t, p$	survival time, recapture constant	3243.9	139.7
$\phi \sim i, p$	survival site, recapture constant	3254.4	150.3
$\phi, p \sim t$	survival constant, recapture time	3274.0	169.9
$\phi \sim S, p \sim S$	survival size, recapture size	3345.2	241.0
$\phi, p$	survival constant, recapture constant	3382.7	278.5

For minimum distance from diver to anemone, we used diver GPS tracks to estimate the minimum distance between a diver and the anemone for each tagged fish in each sample year.

The best model for post-recruitment annual survival  $\phi$  on a log-odds scale has a positive size effect ( $b_a = 0.15 \pm 0.029$  SE) with intercepts varying by site (eqn. B.5,

Fig. B.3). The best model for recapture probability  $p_r$  on a log-odds scale has a negative effect of size ( $b_1 = -0.16 \pm 0.09$  SE) and a negative effect of diver distance from anemone ( $b_2 = -0.15 \pm 0.02$  SE), with intercept  $b_{p_r} = 2.14 \pm 0.87$  SE (eqn. B.6, Fig. B.4), suggesting divers are less likely to recapture larger fish and those at anemones far from areas sampled.

$$\log\left(\frac{\phi}{1-\phi}\right) = b_{\phi_i} + b_a \text{size}. \quad (\text{B.5})$$

$$\log\left(\frac{p_r}{1-p_r}\right) = b_{p_r} + b_1 \text{size} + b_2 d. \quad (\text{B.6})$$

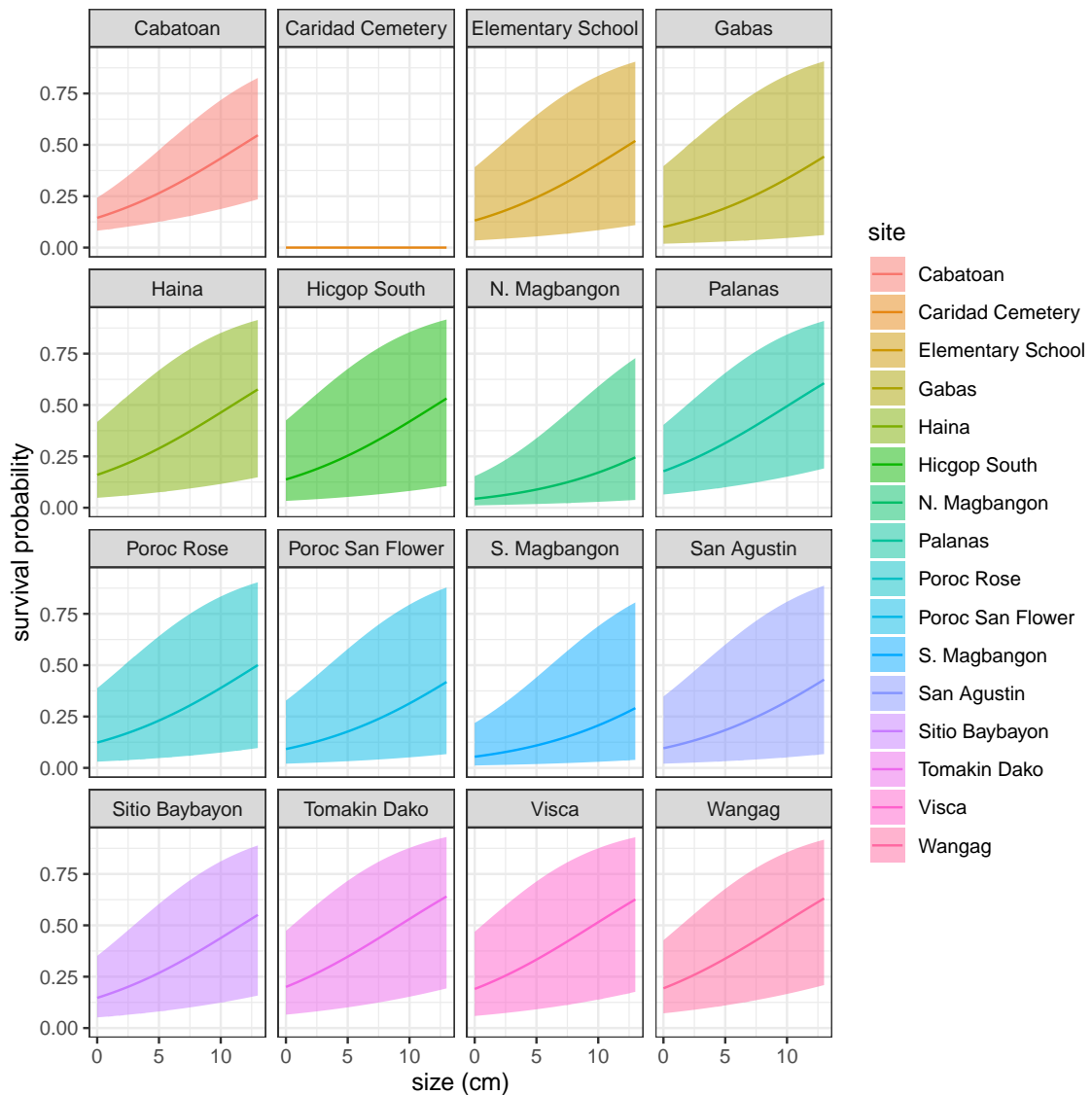


Figure B.3: Annual survival by size at each site.

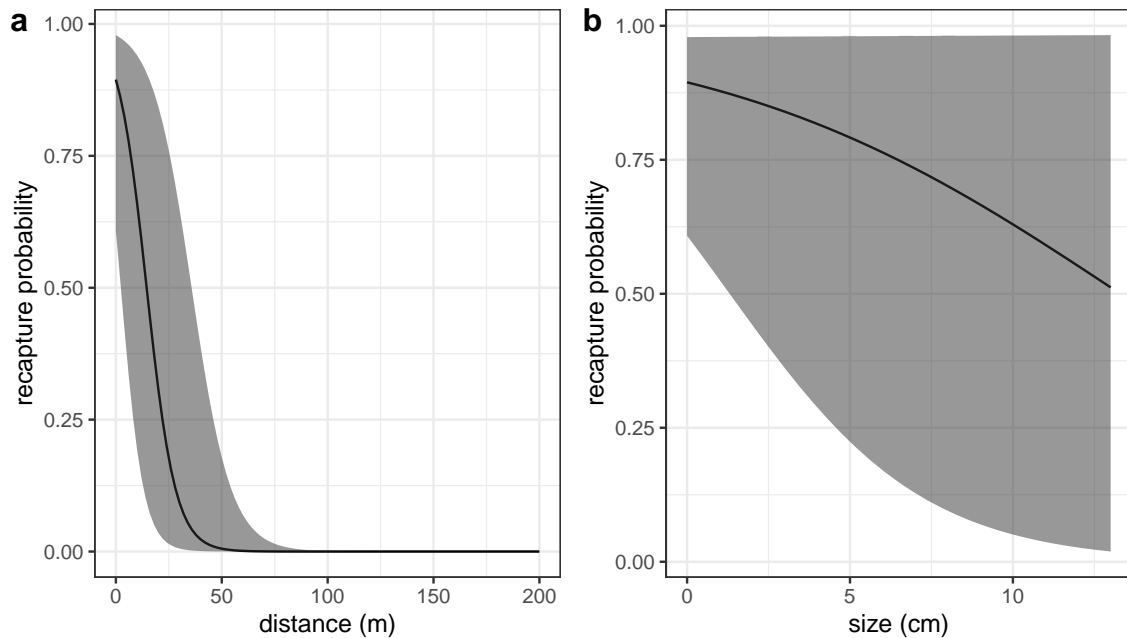


Figure B.4: Effects of a) minimum distance between divers and the anemone where the fish was first caught and b) fish size on the probability the fish will be recaptured, estimated along with survival in a mark-recapture analysis. Size has a slightly negative effect on the probability of recapture - larger fish are stronger swimmers and more likely to flee the anemone when divers approach, but with high uncertainty at larger sizes. Distance also has a negative effect on recapture, as fish tend to stay close to their anemones and are not likely to be recaptured if divers do not get close to their anemone.

## C Result details and sensitivity

### C.1 Abundance trends by site

We use the number of females captured at each site in each sampling year, scaled by the proportion of habitat sampled at that site in that year and by the probability of capturing a fish, to estimate abundance trends for each site (Fig. C.1).

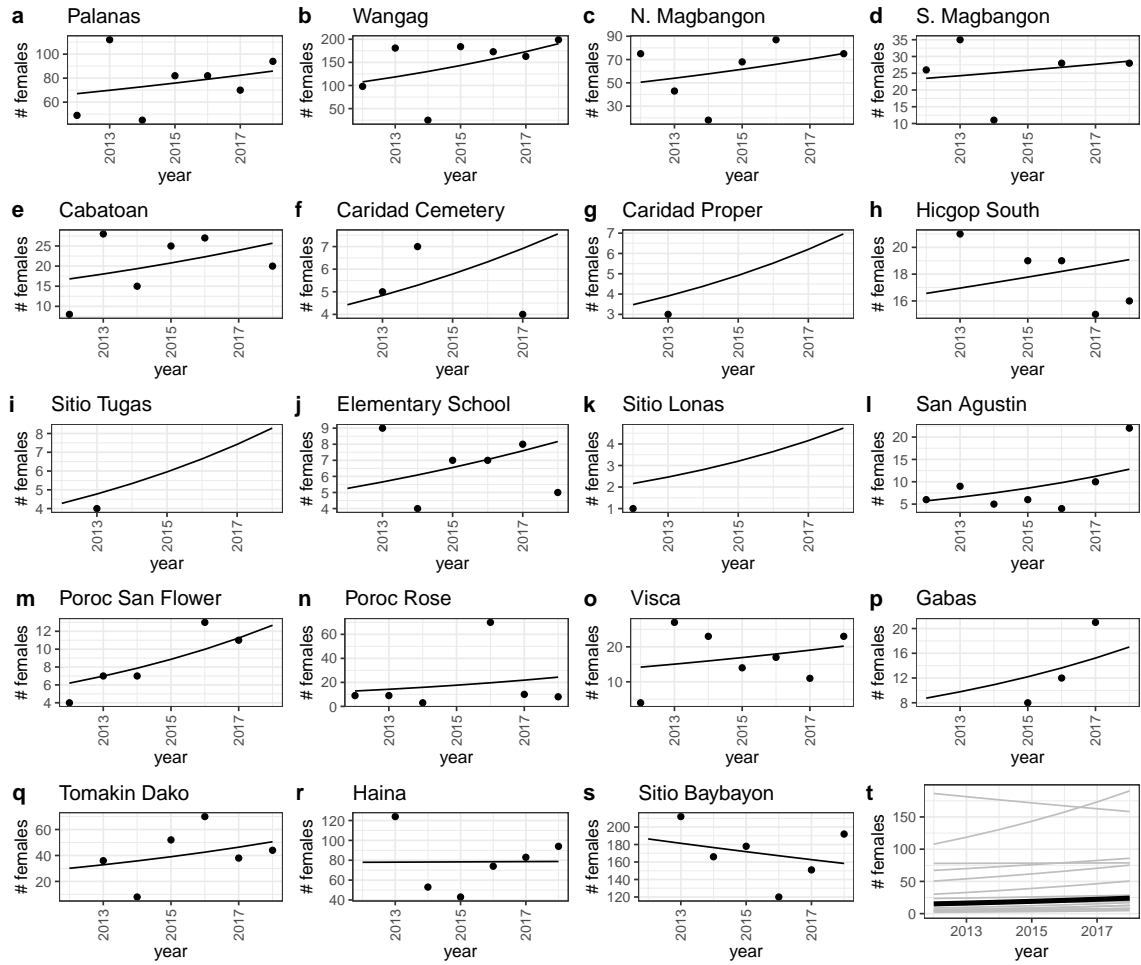


Figure C.1: Scaled number of females captured (black dots) and abundance trends (black lines) by site from a mixed effects model with site as a random effect.

## C.2 Compensating for density dependence

Estimating persistence metrics without compensating for density-dependence in our data gives us an understanding of whether individuals at our sites are able to replace themselves and whether our sites persist as in isolation at the current abundance levels, rather than at low abundance. Without compensation for early life density-dependence, all of our metrics show that the set of sites we sample is less likely to persist as an isolated network. We estimate egg-recruit survival ( $S_e$ ) to be 0.0012 [2.04e-05, 0.008] and average lifetime recruit production (LRP) across sites to be 0.84 [0.36, 4.54], with 55% of LRP estimates  $\geq 1$ . (Fig. C.2c). Our estimate of local replacement (LR), which estimates replacement for recruits from our sites returning to our sites implicitly including dispersal, is 0.10 [0.04, 0.52].

When we calculate LR using all arriving recruits to our sites, however, rather than just those originating there, the best estimate is  $> 1$  (1.22, with 89% of values with uncertainty  $\geq 1$ ), suggesting that there is recruit-recruit replacement at our sites when we include immigrant recruits, even at our current population levels when density-dependence is present.

We do not find any sites with a best estimate or uncertainty range of  $SP \geq 1$  (Figs. C.3a). Our best estimate of the dominant eigenvalue of the realized connectivity matrix  $\lambda_c$  is 0.09 [0.04, 0.90] with 0% of estimates where  $\lambda \geq 1$  (Fig. C.3c).

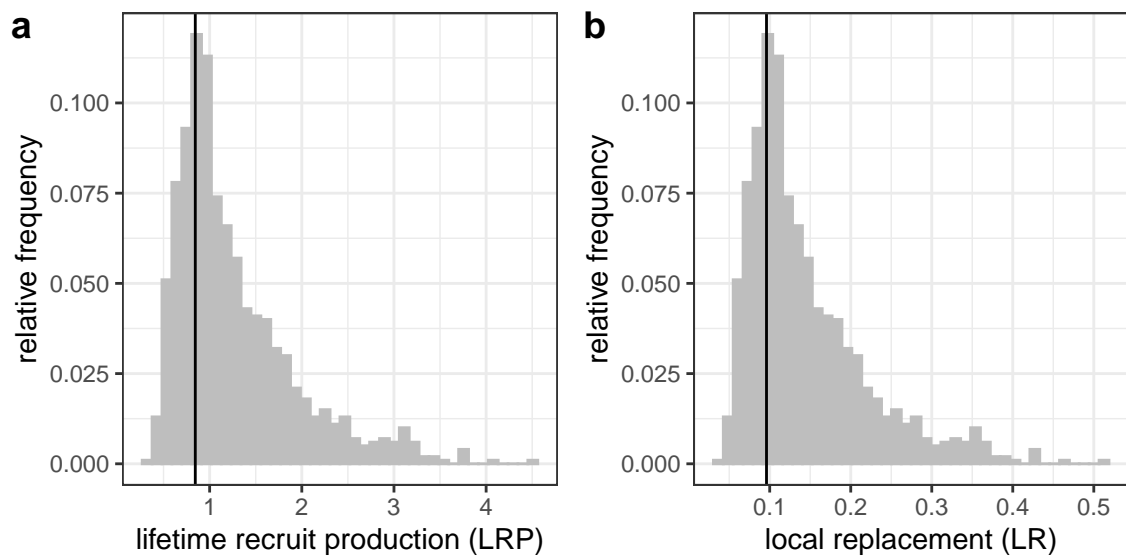


Figure C.2: Estimates of a) LRP, and b) local replacement without compensating for density dependence in early life stages in our data, showing the best estimate (black solid line) and range of estimates considering uncertainty in the inputs. These estimates compare to those in 4c,d, where we correct for additional mortality in early life due to density dependence.

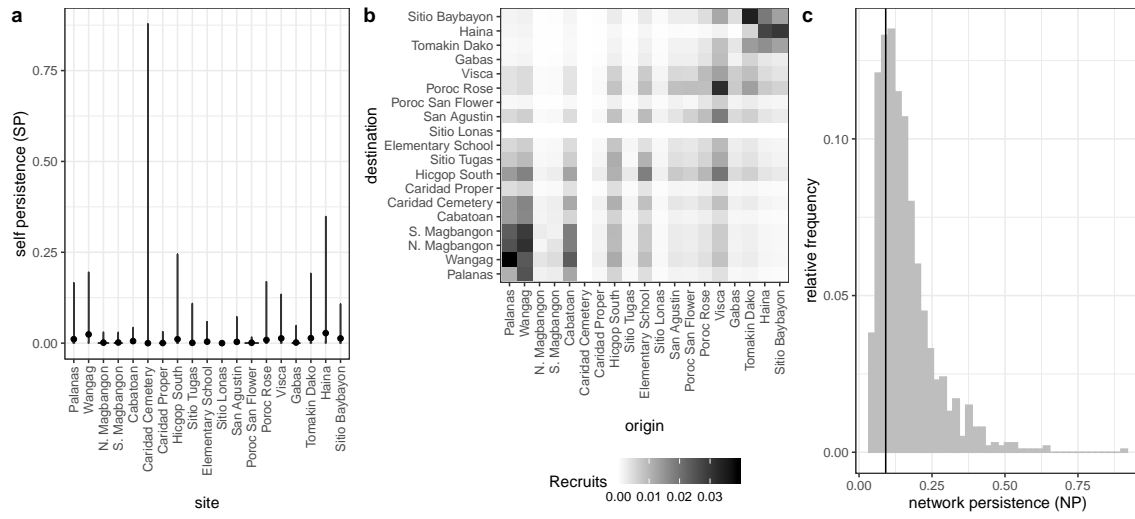


Figure C.3: Values of self-persistence (a), realized connectivity among sites (b), and network persistence (c) without compensation for density-dependence in early life stages in our data. For self-persistence (a) and network persistence (c), the best estimate is shown with in black (point for (a), line for (c)) and the range of estimates considering uncertainty is shown in grey. These estimates compare to those in 5 where we attempt to compensate for density dependence in early life stages.

### C.3 Sensitivity to parameters

The range of parameters not shown in the main text (Fig. 3):

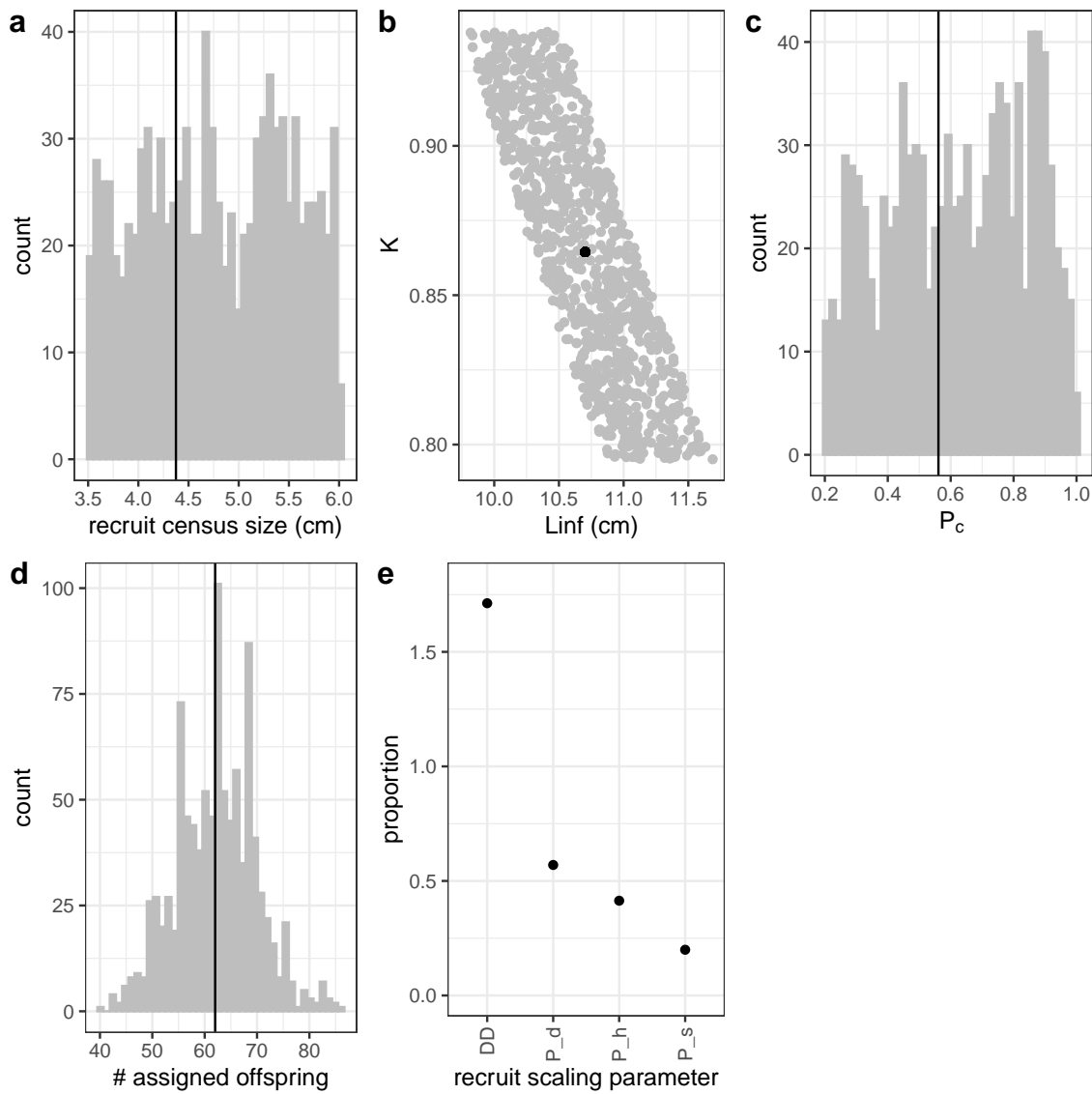


Figure C.4: Range of parameter inputs for uncertainty runs with all uncertainty included, where the black line or point is the value used for the best estimate: a)  $\text{size}_{\text{recruit}}$ , the census size at which fish are considered to have recruited after egg-recruit survival occurs; b) the parameters  $L_{\infty}$  and  $K$  of the von Bertalanffy growth model; c)  $P_c$ , the probability of capturing a fish; d) number of offspring assigned back to parents in the parentage analysis; e) factors that scale the number of estimated recruits from our site based on density-dependence in settler success (DD), proportion of the dispersal kernel captured by our sampling region ( $P_d$ ), the cumulative proportion of our sites we sampled over time ( $P_h$ ), and the proportion of our sampling area that is habitat ( $P_s$ ).

#### C.4 Effects of different types of uncertainty on metrics

Here we show the contribution of uncertainty in each input to the overall uncertainty in the values of LEP (Fig. C.5),  $LRP_{DD}$  (Fig. C.6), egg-recruit survival  $S_{eDD}$  (Fig. C.7), and network persistence  $\lambda_{cDD}$  (Fig. C.8). We calculate the metrics using best estimates for all inputs except the one shown and show the results as violin plots, which show vertical probability densities of the metrics across a range of values.

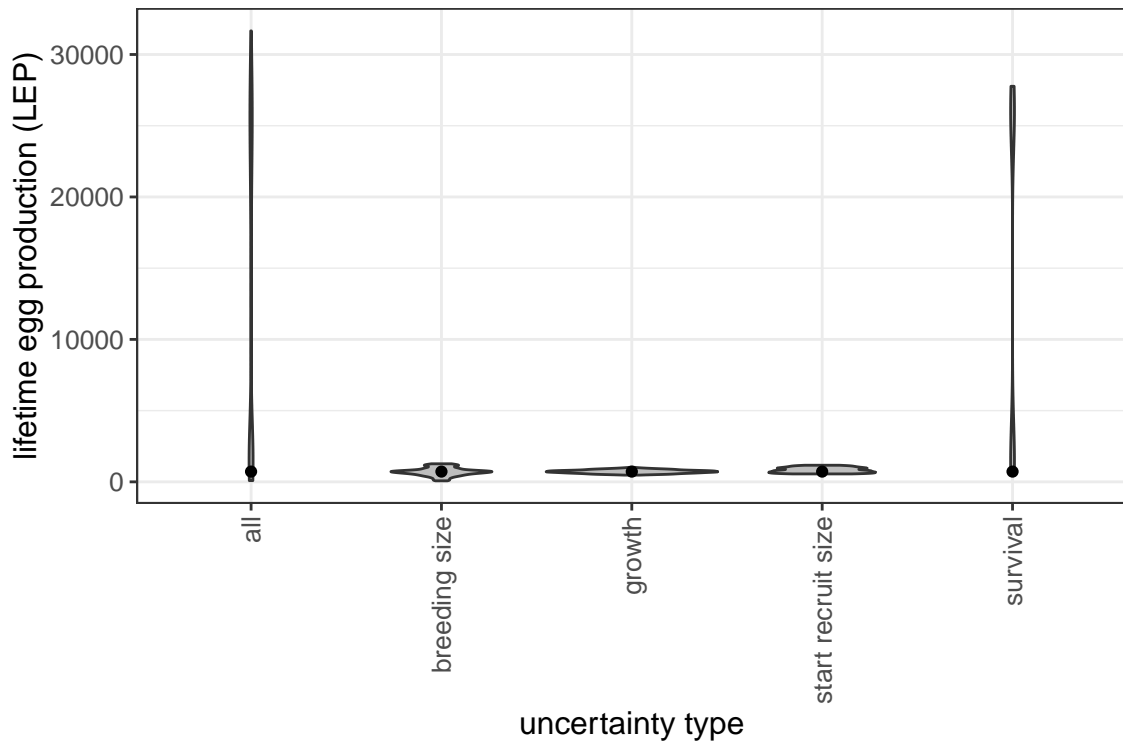


Figure C.5: The contribution of different sources of uncertainty in LEP.

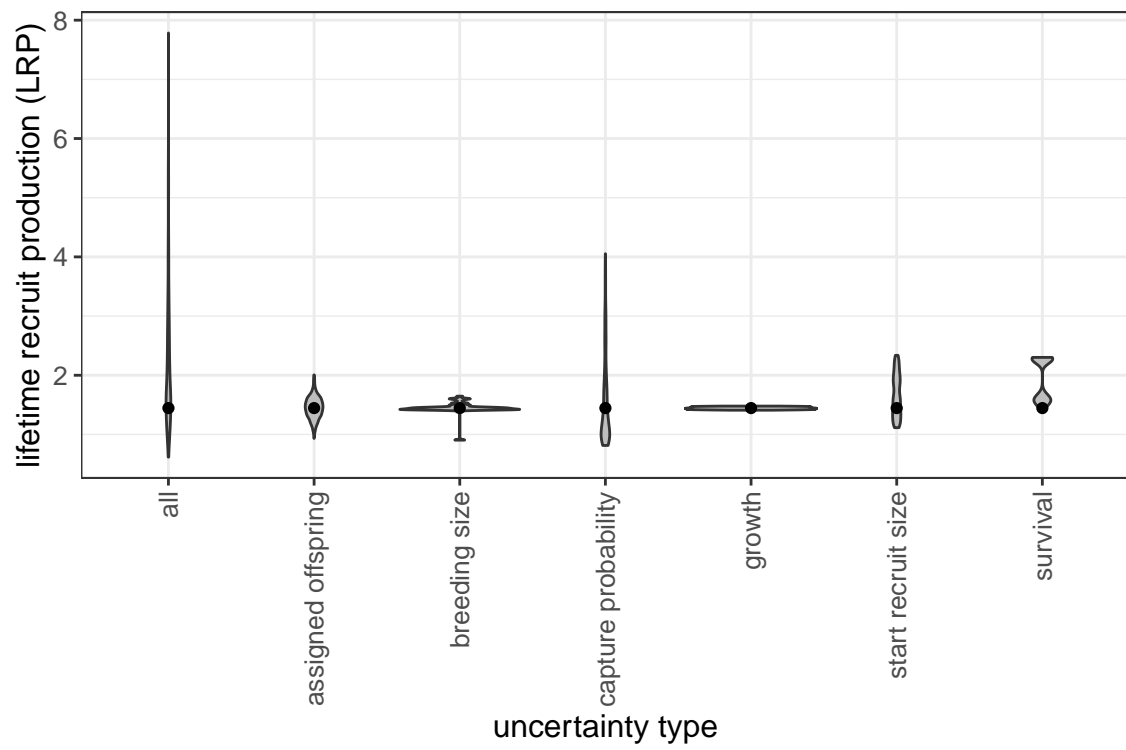


Figure C.6: The contribution of different sources of uncertainty in LRP.

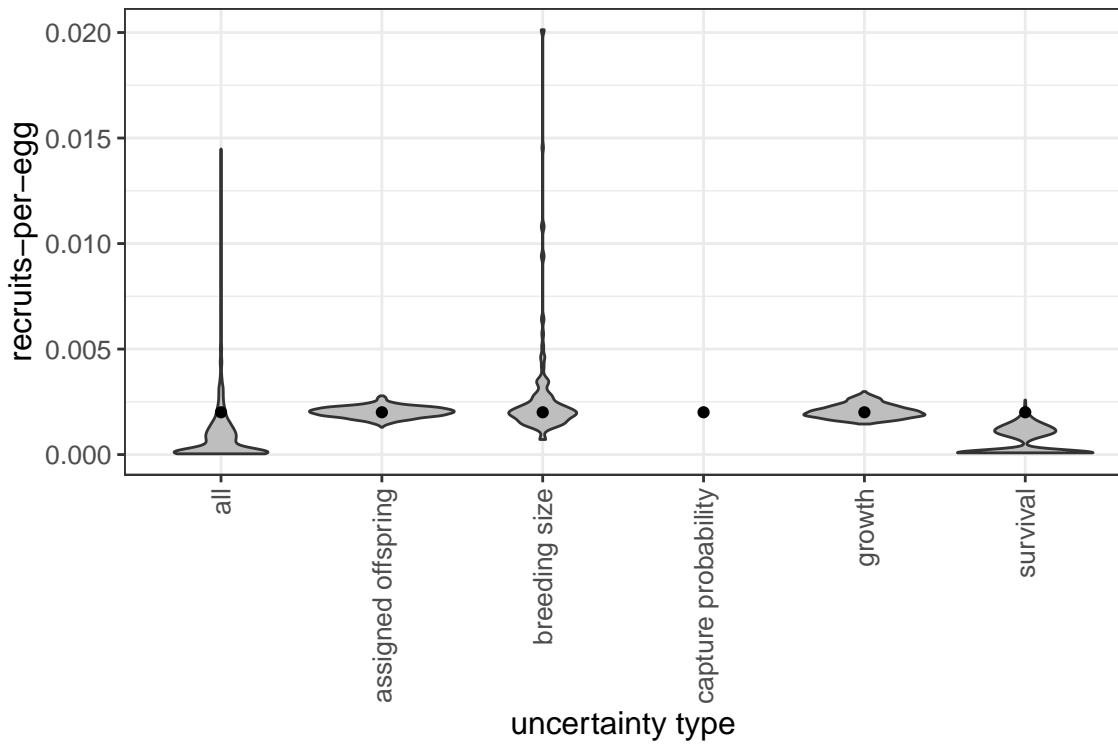


Figure C.7: The contribution of different sources of uncertainty in egg-recruit survival.

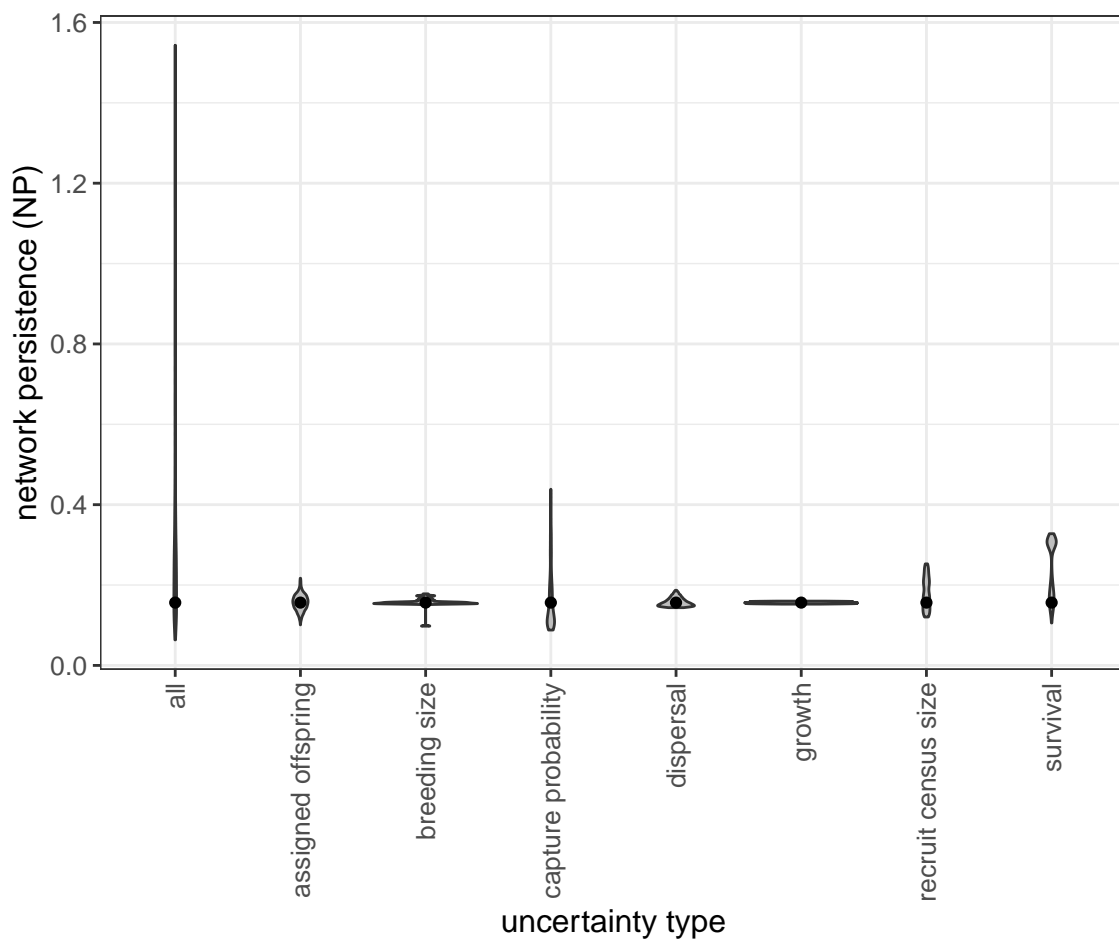


Figure C.8: The contribution of different sources of uncertainty in NP.

## References

- Glenn R Almany, Serge Planes, Simon R Thorrold, Michael L Berumen, Michael Bode, Pablo Saenz-Agudelo, Mary C Bonin, Ashley J Frisch, Hugo B Harrison, Vanessa Messmer, et al. Larval fish dispersal in a coral-reef seascape. *Nature Ecology & Evolution*, 1:0148, 2017.
- Michael Arvedlund, Mark I McCormick, Daphne G Fautin, and Mogens Bildsøe. Host recognition and possible imprinting in the anemonefish *amphiprion melanopus* (pisces: Pomacentridae). *Marine Ecology Progress Series*, 188:207–218, 1999.
- Diana S Baetscher, Eric C Anderson, Elizabeth A Gilbert-Horvath, Daniel P Malone, Emily T Saarman, Mark H Carr, and John Carlos Garza. Dispersal of a nearshore marine fish connects marine reserves and adjacent fished areas along an open coast. *Molecular ecology*, 28(7):1611–1623, 2019.
- Douglas Bates, Martin Mächler, Ben Bolker, and Steve Walker. Fitting linear mixed-effects models using lme4. *Journal of Statistical Software*, 67(1):1–48, 2015. doi: 10.18637/jss.v067.i01.
- David R Bellwood and Rebecca Fisher. Relative swimming speeds in reef fish larvae. *Marine Ecology Progress Series*, 211:299–303, 2001.
- Michael Bode, David H Williamson, Hugo B Harrison, Nick Outram, and Geoffrey P Jones. Estimating dispersal kernels using genetic parentage data. *Methods in Ecology and Evolution*, 9(3):490–501, 2018.

Michael Bode, Jeffrey M. Leis, Luciano B. Mason, David H. Williamson, Hugo B. Harrison, Severine Choukroun, and Geoffrey P. Jones. Successful validation of a larval dispersal model using genetic parentage data. *PLOS Biology*, 17(7):1–13, 07 2019. doi: 10.1371/journal.pbio.3000380. URL <https://doi.org/10.1371/journal.pbio.3000380>.

Louis W. Botsford, Alan Hastings, and Steven D. Gaines. Dependence of sustainability on the configuration of marine reserves and larval dispersal distance. *Ecology Letters*, 4:144–150, 2001.

Louis W Botsford, J Wilson White, and Alan Hastings. *Population Dynamics for Conservation*. Oxford University Press, 2019.

Scott C Burgess, Kerry J Nickols, Chris D Griesemer, Lewis AK Barnett, Allison G Dedrick, Erin V Satterthwaite, Lauren Yamane, Steven G Morgan, J Wilson White, and Louis W Botsford. Beyond connectivity: how empirical methods can quantify population persistence to improve marine protected-area design. *Ecological Applications*, 24(2):257–270, 2014.

Peter Buston. Forcible eviction and prevention of recruitment in the clown anemonefish. *Behavioral Ecology*, 14(4):576–582, 2003a.

Peter Buston. Social hierarchies: size and growth modification in clownfish. *Nature*, 424(6945):145–146, 2003b.

Peter M Buston and Cassidy C DAloia. Marine ecology: reaping the benefits of local dispersal. *Current Biology*, 23(9):R351–R353, 2013.

Peter M Buston and Jane Elith. Determinants of reproductive success in dominant pairs of clownfish: a boosted regression tree analysis. *Journal of Animal Ecology*, 80(3):528–538, 2011.

Peter M Buston, Geoffrey P Jones, Serge Planes, and Simon R Thorrold. Probability of successful larval dispersal declines fivefold over 1 km in a coral reef fish. *Proceedings of the Royal Society of London B: Biological Sciences*, page rspb20112041, 2011.

Henry S Carson, Geoffrey S Cook, Paola C López-Duarte, and Lisa A Levin. Evaluating the importance of demographic connectivity in a marine metapopulation. *Ecology*, 92(10):1972–1984, 2011.

Hal Caswell. *Matrix population models: construction, analysis, and interpretation*. Sinauer Associates Inc., Sunderland, Massachusetts, 2nd edition, 2001.

Katrina A Catalano, Allison G Dedrick, Michelle Stuart, Jonathan Purtiz, Humberto Montes, Jr., and Malin Pinsky. Interannual variability of genetic connectivity in a coral reef fish *Amphiprion clarkii*. in prep.

MA Coleman, P Cetina-Heredia, M Roughan, M Feng, E van Sebille, and BP Kehler. Anticipating changes to future connectivity within a network of marine protected areas. *Global Change Biology*, 2017.

C. C. D'Aloia, S. M. Bogdanowicz, J. E. Majoris, R. G. Harrison, and P. M. Buston. Self-recruitment in a Caribbean reef fish: a method for approximating dispersal

kernels accounting for seascape. *Molecular Ecology*, 22(9):2563–2572, May 2013. ISSN 09621083. doi: 10.1111/mec.12274. URL <http://doi.wiley.com/10.1111/mec.12274>.

Cassidy C Daloia, Steven M Bogdanowicz, Robin K Francis, John E Majoris, Richard G Harrison, and Peter M Buston. Patterns, causes, and consequences of marine larval dispersal. *Proceedings of the National Academy of Sciences*, 112(45):13940–13945, 2015.

JK Elliott, JM Elliott, and RN Mariscal. Host selection, location, and association behaviors of anemonefishes in field settlement experiments. *Marine Biology*, 122(3):377–389, 1995.

Stephen P Ellner, Dylan Z Childs, Mark Rees, et al. Data-driven modelling of structured populations. *A practical guide to the Integral Projection Model*. Cham: Springer, 2016.

Augustus J. Fabens. Properties and fitting of the von bertalanffy growth curve. *Growth*, 29:265–289, 1965.

Lenore Fahrig. How much habitat is enough? *Biological conservation*, 100(1):65–74, 2001.

Daphne Gail Fautin, Gerald R Allen, Gerald Robert Allen, Australia Naturalist, Gerald Robert Allen, and Australie Naturaliste. Field guide to anemonefishes and their host sea anemones. 1992.

Will F Figueira. Connectivity or demography: defining sources and sinks in coral reef fish metapopulations. *Ecological Modelling*, 220(8):1126–1137, 2009.

Rebecca Fisher. Swimming speeds of larval coral reef fishes: impacts on self-recruitment and dispersal. *Marine Ecology Progress Series*, 285:223–232, 2005.

Emma Fuller, Eleanor Brush, and Malin L Pinsky. The persistence of populations facing climate shifts and harvest. *Ecosphere*, 6(9):1–16, 2015.

Lysel Garavelli, J Wilson White, Iliana Chollett, and Laurent Marcel Chérubin. Population models reveal unexpected patterns of local persistence despite widespread larval dispersal in a highly exploited species. *Conservation Letters*, 11(5):e12567, 2018.

Sarah O Hameed, J Wilson White, Seth H Miller, Kerry J Nickols, and Steven G Morgan. Inverse approach to estimating larval dispersal reveals limited population connectivity along 700 km of wave-swept open coast. *Proceedings of the Royal Society B: Biological Sciences*, 283(1833):20160370, 2016.

Ilkka Hanski. Metapopulation dynamics. *Nature*, 396(6706):41–49, 1998.

Hugo B Harrison, David H Williamson, Richard D Evans, Glenn R Almany, Simon R Thorrold, Garry R Russ, Kevin A Feldheim, Lynne Van Herwerden, Serge Planes, Maya Srinivasan, et al. Larval export from marine reserves and the recruitment benefit for fish and fisheries. *Current biology*, 22(11):1023–1028, 2012.

Deborah R Hart and Antonie S Chute. Estimating von bertalanffy growth parameters

from growth increment data using a linear mixed-effects model, with an application to the sea scallop *placopecten magellanicus*. *ICES Journal of Marine Science*, 66(10):2165–2175, 2009.

Alan Hastings and Louis W. Botsford. Persistence of spatial populations depends on returning home. *Proceedings of the National Academy of Sciences*, 103:6067–6072, 2006.

Akihisa Hattori and Yasunobu Yanagisawa. Life-history pathways in relation to gonadal sex differentiation in the anemonefish, *amphiprion clarkii*, in temperate waters of japan. *Environmental Biology of Fishes*, 31(2):139–155, 1991.

Kina Hayashi, Katsunori Tachihara, and James Davis Reimer. Low density populations of anemonefish with low replenishment rates on a reef edge with anthropogenic impacts. *Environmental Biology of Fishes*, 102(1):41–54, 2019.

Jordan N. Holtswarth, Shem B. San Jose, Humberto R. Montes Jr., James W. Morley, and Malin. L Pinsky. The reproductive seasonality and fecundity of yellowtail clownfish (*amphiprion clarkii*) off the philippines. *Bulletin of Marine Science*, 93, 2017.

Darren W Johnson, Mark R Christie, Timothy J Pusack, Christopher D Stallings, and Mark A Hixon. Integrating larval connectivity with local demography reveals regional dynamics of a marine metapopulation. *Ecology*, 99(6):1419–1429, 2018.

David M. Kaplan, Louis W. Botsford, Michael R. O’Farrell, Steven D. Gaines, and Salvador Jorgensen. Model-based assessment of persistence in proposed marine

protected area designs. *Ecological Applications*, 19(2):433–448, March 2009. ISSN 1051-0761. doi: 10.1890/07-1705.1. URL <http://www.esajournals.org/doi/abs/10.1890/07-1705.1>.

J.L. Laake. RMark: An r interface for analysis of capture-recapture data with MARK. AFSC Processed Rep. 2013-01, Alaska Fish. Sci. Cent., NOAA, Natl. Mar. Fish. Serv., Seattle, WA, 2013. URL <http://www.afsc.noaa.gov/Publications/ProcRpt/PR2013-01.pdf>.

David Lecchini, Serge Planes, and René Galzin. Experimental assessment of sensory modalities of coral-reef fish larvae in the recognition of their settlement habitat. *Behavioral Ecology and Sociobiology*, 58(1):18–26, 2005.

Dale R Lockwood, Alan Hastings, and Louis W Botsford. The effects of dispersal patterns on marine reserves: does the tail wag the dog? *Theoretical population biology*, 61(3):297–309, 2002.

Haruki Ochi. Mating behavior and sex change of the anemonefish, *amphiprion clarkii*, in the temperate waters of southern japan. *Environmental Biology of Fishes*, 26(4):257–275, 1989.

Malin L Pinsky, Humberto R Montes Jr, and Stephen R Palumbi. Using isolation by distance and effective density to estimate dispersal scales in anemonefish. *Evolution*, 64(9):2688–2700, 2010.

BJ Puckett and DB Eggleston. Metapopulation dynamics guide marine reserve de-

sign: importance of connectivity, demographics, and stock enhancement. *Ecosphere*, 7(6), 2016.

H Ronald Pulliam. Sources, sinks, and population regulation. *The American Naturalist*, 132(5):652–661, 1988.

Océane C Salles, Glenn R Almany, Michael L Berumen, Geoffrey P Jones, Pablo Saenz-Agudelo, Maya Srinivasan, Simon R Thorrold, Benoit Pujol, and Serge Planes. Strong habitat and weak genetic effects shape the lifetime reproductive success in a wild clownfish population. *Ecology letters*, 23(2):265–273, 2020.

Océane C. Salles, Jeffrey A. Maynard, Marc Joannides, Corentin M. Barbu, Pablo Saenz-Agudelo, Glenn R. Almany, Michael L. Berumen, Simon R. Thorrold, Geoffrey P. Jones, and Serge Planes. Coral reef fish populations can persist without immigration. *Proceedings of the Royal Society B: Biological Sciences*, 282(1819): 20151311, November 2015. ISSN 0962-8452, 1471-2954. doi: 10.1098/rspb.2015.1311. URL <http://rspb.royalsocietypublishing.org/lookup/doi/10.1098/rspb.2015.1311>.

James NM Smith and Jessica J Hellmann. Population persistence in fragmented landscapes. *Trends in Ecology & Evolution*, 17(9):397–399, 2002.

Diane M Thompson, J Kleypas, F Castruccio, Enrique N Curchitser, Malin L Pinsky, B Jönsson, and James R Watson. Variability in oceanographic barriers to coral larval dispersal: Do currents shape biodiversity? *Progress in oceanography*, 165: 110–122, 2018.

Nick Tolimieri and Phillip S Levin. The roles of fishing and climate in the population dynamics of bocaccio rockfish. *Ecological Applications*, 15(2):458–468, 2005.

Jinliang Wang. Sibship reconstruction from genetic data with typing errors. *Genetics*, 166(4):1963–1979, 2004.

Jinliang Wang. Estimation of migration rates from marker-based parentage analysis. *Molecular ecology*, 23(13):3191–3213, 2014.

J. Wilson White, Mark H Carr, Jennifer E Caselle, Libe Washburn, C. Brock Woodson, Stephen R Palumbi, Peter M Carlson, Robert R Warner, Bruce A Menge, John A Barth, Carol A Blanchette, Peter T Raimondi, and Kristen Milligan. Connectivity, dispersal, and recruitment: Connecting benthic communities and the coastal ocean. *Oceanography*, 32(3):50–59, 2019.

Jw White, Lw Botsford, A Hastings, and Jl Largier. Population persistence in marine reserve networks: incorporating spatial heterogeneities in larval dispersal. *Marine Ecology Progress Series*, 398:49–67, January 2010. ISSN 0171-8630, 1616-1599. doi: 10.3354/meps08327. URL <http://www.int-res.com/abstracts/meps/v398/p49-67/>.

Adam Yawdoszyn. Fecundity in clownfish. in prep.